AD-A274 014

(2)

ARMY RESEARCH LABORATORY

Determination of Fracture Stress and Effective Crack Tip Radius From Toughness (K_{Ic}) and Yield Strength (Y)

Reinier Beeuwkes, Jr.

ARL-SR-3

November 1993

Approved for public release; distribution unlimited.

REPORT DOCUMENTATION PAGE

Form Approved OMB No. 0704-0188

1. AGENCY USE ONLY *(Leave blank)*

2. REPORT DATE
November 1993

3. REPORT TYPE AND DATES COVERED
Final Report

4. TITLE AND SUBTITLE
Determination of Fracture Stress and Effective Crack Tip Radius from Toughness (K_{Ic}) and Yield Strength (Y)

5. FUNDING NUMBERS

6. AUTHOR(S)
Reinier Beeuwkes, Jr.

7. PERFORMING ORGANIZATION NAME(S) AND ADDRESS(ES)
U.S. Army Research Laboratory
Watertown, Massachusetts 02172-0001
ATTN: AMSRL-MA-D

8. PERFORMING ORGANIZATION REPORT NUMBER
ARL-SR-3

9. SPONSORING/MONITORING AGENCY NAME(S) AND ADDRESS(ES)
U.S. Army Research Laboratory
2800 Powder Mill Road
Adelphi, Maryland 20783-1197

10. SPONSORING/MONITORING AGENCY REPORT NUMBER

11. SUPPLEMENTARY NOTES

12a. DISTRIBUTION/AVAILABILITY STATEMENT
Approved for public release; distribution unlimited.

12b. DISTRIBUTION CODE

13. ABSTRACT *(Maximum 200 words)*

This is the last of several reports in which K_{Ic} toughness is not considered basic, but dependent on two metallurgically controllable parameters, the tensile nil-ductility fracture stress and an effective crack tip radius formed by straining at the sharp crack tip which is shown by examples not to be uniquely dependent on load as would the mathematical increase in radius of a rounded tip no matter how small, in a homogeneous material but also dependent metallurgically on micromechanical structure. The reports describe how to determine the fracture stress and the radius from K_{Ic} tests with the aid of a postulated fracture criterion characteristic of the material and a curve derived from the solution for the state of stress in the yielded region of a short elliptically shaped flat crack lying across the center of a plate under uniform tensile loading. Here a more exact solution by Colin E. Freese and Dennis M. Tracey supplants the approximate ones used previously and it is shown that dependent on tempering or test temperature, radius determinations remain unchanged to 20% larger although fracture stress determinations are 75% to 85% as large. The state of application and advantages of the fracture stress approach over the energy approach are discussed by showing how usual K_{Ic} determinations may be modified to handle cases where a hydrostatic pressure is superimposed on the usual loading.

14. SUBJECT TERMS
Fracture mechanics

15. NUMBER OF PAGES
61

16. PRICE CODE

17. SECURITY CLASSIFICATION OF REPORT	18. SECURITY CLASSIFICATION OF THIS PAGE	19. SECURITY CLASSIFICATION OF ABSTRACT	20. LIMITATION OF ABSTRACT
Unclassified	Unclassified	Unclassified	UL

NSN 7540-01-280-5500

Standard Form 298 (Rev. 2-89)
Prescribed by ANSI Std. Z39-18
298-102

CONTENTS

	Page
INTRODUCTION	1
FINITE ELEMENT DATA AND MATCHING FORMULAE	4
Matching Formulae	7
BRITTLE (NIL-DUCTILITY) TENSILE FRACTURE STRESS, EFFECTIVE RADIUS, YIELD STRENGTH	8
Fracture Stress	8
Radius	10
Yield Strength	11
USE OF THE FINITE ELEMENT DATA	12
Mode I Standard Test K_{Ic} Data	12
HYDROSTATIC PRESSURE MODIFICATION OF K_{Ic}	16
QUANTITATIVE RELATIONSHIP BETWEEN THE FINITE ELEMENT AND FIRST REPORT RESULTS	18
L Versus Δ	18
$F = (1 + \beta)Y + f$ vs. Δ	20
DISCUSSION AND CONCLUSIONS	24
ACKNOWLEDGMENTS	34
APPENDIX I: TRANSPARENT OVERLAYS	47
APPENDIX II: ENERGY RELATIONS IN SUPERPOSITION OF HYDROSTATIC PRESSURE	51
REFERENCES	55

Figures

Page

1. Transverse View of Mid-Thickness Slice Showing Fracture Origin ac Elastic-Plastic Boundary and Slip Lines. ρ =0.005 in. 350x. 35
2. Parabolic Crack - Partial Plasticity, General Features. 36
3. L versus Δ. Freese - Tracey Data. 37
4. Δ versus x/ρ. Freese - Tracey Data 38
5. M versus with Matching Curve. Freese - Tracey Data 39
6. True Stress - True Strain Curves for Annealed Tungsten. Test Temperature 523°K. From Bechtold Data. 40
7. Meaning of Fracture Stress. 41
8. Influence of Sulfur on Plane - Strain Fracture Toughness of 0.45C Ni-Cr-Mo Steels 42
9. Brittleness: Stress Concentration, k, to Cause Failure, $e=0^+$ 43
10. (1/ Δ L) versus (1/ Δ) on ln ln Paper. Freese - Tracey Data 44
11. Constant f Overlay. 45
12. Constant F Overlay. 46

Tables

I. Nomenclature and Basic Relations. 5

II. Dimensionless Quantities Computed from Freese-Tracey Data for an Elliptical Crack in a Tensile Specimen 6

INTRODUCTION

This is the last of several[1-4] reports which conceptually go beyond the usual practical treatments of K_{Ic} in the theoretical applied mechanics literature. That literature consists of derivations of a K_{Ic} or other single associated measure (COD), for each of many configurations of cracked material and loading such that evaluation of the appropriate formula to any test under K_{Ic} conditions gives the same toughness value as would a similar test of any other configuration of the same material. This is consistent with the notion that toughness is a unique fundamental property of materials, one not made up of simple fundamental quantities such as fracture stress or work hardening modulus. Here, however, K_{Ic} toughness is not considered basic but dependent on two metallurgically controllable parameters, the tensile brittle fracture stress and a postulated strain parameter, the effective crack tip radius existing at the K_{Ic} fracture load stress; this, in turn, is considered to be dependent on metallurgy, e.g., sulfur content, as well as the K_{Ic} loading stress. The reports describe how to determine the fracture stress and the radius from K_{Ic} tests using a postulated fracture criterion characteristic of the material and a curve derived from the solution for the state of stress in the yielded region of a short elliptically shaped flat crack lying across the center of a plate under uniform tensile loading. Here a more exact solution supplants the approximate ones used previously and it is shown that radius determinations remain unchanged although fracture stress determinations are 75% as large. The state of application and advantages of the fracture stress approach over the energy approach are discussed.

The title of this report was first used on a report[4] issued in October 1978; for comparison that report shall be called the First Report. It was a "how to" report based upon a curve obtained by an approximate analysis employing elasticity shear stress trajectories with the hope that the analysis would soon be followed* by a more exact finite element one [5,6]. The latter was expected to apply, not only to the crack problem, but to evaluate the approximate type of analysis for the crack and other stress concentration problems where the yield point was locally exceeded and for which an exact analysis was difficult to achieve.

A careful, time consuming finite element analysis was finally made in 1984 by Colin E. Freese and Dennis M. Tracey largely in answer to the above expectation[7-10]. It is the one used in this report, is considered very good (the best available), and contains a surprising limiting stress result. However, it leaves some important questions unanswered: whether the stress is maximum just off the center line of the crack, as found by the

*It was followed by a stimulating finite element and experimental analysis led by Albert Kobayashi (References 5, 6). The experimental results were very satisfactory, but it was evident that a finer grid would be necessary for precise finite element results.

approximate method (a distance too small for the finite elements used) and whether it is appropriate, even near the crack tip, to compare the approximation which was based upon the uniform biaxial loading used by fracture mechanics pioneers, following Griffith[11,12], with the uniaxial tension loading used by Freese and Tracey. The delay in publishing the present analysis was largely due to the expectation that time could have been found for definitive answers to such questions.

The approach here to crack toughness or brittleness is not an energy approach but a tensile brittle fracture stress[14] approach (Fig.1). Using shear stress trajectories (Fig. 2), the maximum tensile stress, S_m for loading stress S, is computed from $S_m = Y (1 + \Delta)$ where Y is the plane strain yield strength and Δ is the largest angle change found among all the principal shear stress trajectories crossing the yield region at the crack tip. Thus, this stress is ahead of the crack and increases with the amount of yielding; hence, load; if it equals the brittle fracture stress, F, of the material, failure occurs. The strain where the trajectory corresponding to Δ crosses the yield region is small; hence, work hardening is negligible, and since the trajectory is far from the crack tip with any appreciable Δ, the exact shape of the tip is of limited importance; the radius of the tip found from the analysis, whatever its origin, is an effective radius.

The finite element solution is based upon a crack tip radius of $\rho = 0.001$, taking half the crack length as the unit of distance, and was applied to other cases through dimensionless ratios. For that solution, the dimensionless ratio Δ was computed by equating $Y\ (1 + \Delta)$ to the maximum stress corresponding to an applied loading stress. Y, the plane strain yield strength, was taken to be $2\times10^5/\sqrt{3}$.

FINITE ELEMENT DATA AND MATCHING FORMULAE

Our notation and definitions are contained in Table I.

The finite element program models a long flat tensile specimen which is loaded uniformly at the ends and is pierced by a central crack of length 2a across its middle.

For present use, Freese supplied the unsmoothed finite element method results, as well as L, M, and Δ directly computed from it, by Table II. The L and M versus Δ data is used to determine fracture stress F, and effective crack tip radius, ρ, from appropriate (pressure free crack surface) experimental K_{Ic}, Y (toughness, yield strength) data.

TABLE I
NONEMCLATURE AND BASIC RELATIONS

a = crack length/2

ρ = 0.001 = crack tip radius in Table II

Y_t = Tensile test yield strength = 10^2 ksi in Table II

Y = $2Y_t/\sqrt{3}$ = Plane strain yield strength, the yield strength used in all analyses in this report.

S = The uniform tensile loading stress

x = Distance from crack tip to point of maximum stress, S_m

S_m = Maximum stress ahead of crack at loading stress S, i.e., stress at x.

F = Tensile stress needed to cause fracture; here the nil-ductility tensile fracture stress.

S_m = F under K_{Ic} test conditions.

Δ = Maximum shear stress trajectory angle change;

$$S_m = Y(1 + \Delta)$$

L = $Y/S\sqrt{a\rho}$

= $Y\sqrt{\pi\rho}/K$, a dimensionless parameter

= 3.65148/S in Table II; at initial yielding L = 2

K = $S\sqrt{\pi a}$ here, = K_{Ic} toughness under K_{Ic} test conditions

M = $L\sqrt{x/\rho} \equiv (Y/K)\sqrt{\pi x}$, by definition.

$\rho = 0.001;\ a = 1$
$Y_t = 100\,ksi;\ Y = (2/\sqrt{3})\,Y_t$
$S = Loading Stress$
$S_m = Maximum\ S;\ S\ at\ x$

$K = S\sqrt{\pi a}$
$L = Y/S\sqrt{a/\rho} = Y\sqrt{\pi\rho}/K$
$M = L\sqrt{x/\rho} = Y\sqrt{\pi x}/K$
$\Delta = S_m/Y - 1$

INITIAL YIELD:
$Y = S(1 + 2\sqrt{a/\rho})$
$\approx 2S\sqrt{a/\rho}$, *i.e.*,
$L = 2$

x/ρ	S_m/Y_t	S	L	Δ	$1/\Delta$	$1/\Delta L$	M	$1/(\Delta+1)$	$1/[(\Delta+1)L]$
0.90952E-01	0.10115E+01	0.18162E+01	0.20105E+01	-0.12402E+00	-0.80635E+01	-0.40107E+01	0.60633E+00	0.11416E+01	0.56780E+00
0.90952E-01	0.11984E+01	0.22589E+01	0.16165E+01	0.37845E-01	0.26424E+02	0.16346E+02	0.48750E+00	0.96354E+00	0.59607E+00
0.16683E+00	0.12594E+01	0.25966E+01	0.14063E+01	0.90672E-01	0.11029E+02	0.78426E+01	0.57438E+00	0.91687E+00	0.65199E+00
0.22103E+00	0.13648E+01	0.29333E+01	0.12448E+01	0.18195E+00	0.54960E+01	0.44150E+01	0.58525E+00	0.84606E+00	0.67965E+00
0.25897E+00	0.13742E+01	0.31700E+01	0.11518E+01	0.19009E+00	0.52606E+01	0.45669E+01	0.58619E+00	0.84027E+00	0.72947E+00
0.35653E+00	0.14037E+01	0.33959E+01	0.10753E+01	0.21564E+00	0.46374E+01	0.43128E+01	0.64204E+00	0.82261E+00	0.76503E+00
0.45408E+00	0.14929E+01	0.36930E+01	0.98876E+00	0.29289E+00	0.34143E+01	0.34531E+01	0.66628E+00	0.77346E+00	0.78226E+00
0.47576E+00	0.15142E+01	0.39236E+01	0.93065E+00	0.31134E+00	0.32120E+01	0.34513E+01	0.64102E+00	0.76258E+00	0.81941E+00
0.52454E+00	0.15375E+01	0.41756E+01	0.87448E+00	0.33151E+00	0.30165E+01	0.34494E+01	0.63334E+00	0.75102E+00	0.85882E+00
0.66546E+00	0.16023E+01	0.44645E+01	0.81789E+00	0.38763E+00	0.25798E+01	0.31542E+01	0.66720E+00	0.72065E+00	0.88111E+00
0.70340E+00	0.16400E+01	0.47457E+01	0.76943E+00	0.42028E+00	0.23794E+01	0.30924E+01	0.64531E+00	0.70409E+00	0.91507E+00
0.74134E+00	0.16636E+01	0.50128E+01	0.72865E+00	0.44072E+00	0.22690E+01	0.31144E+01	0.62729E+00	0.69410E+00	0.95271E+00
0.83348E+00	0.16904E+01	0.52839E+01	0.69106E+00	0.46383E+00	0.21556E+01	0.31191E+01	0.63090E+00	0.68309E+00	0.98847E+00
0.95271E+00	0.17440E+01	0.55870E+01	0.65357E+00	0.51035E+00	0.19594E+01	0.29981E+01	0.63703E+00	0.66210E+00	0.10131E+01
0.98523E+00	0.17684E+01	0.58536E+01	0.62380E+00	0.53148E+00	0.18815E+01	0.30162E+01	0.61918E+00	0.65296E+00	0.10467E+01
0.10394E+01	0.17909E+01	0.61447E+01	0.59425E+00	0.55096E+00	0.18150E+01	0.30543E+01	0.60584E+00	0.64476E+00	0.10850E+01
0.11803E+01	0.18207E+01	0.64591E+01	0.56632E+00	0.57677E+00	0.17338E+01	0.30669E+01	0.61418E+00	0.63481E+00	0.11218E+01
0.12671E+01	0.18583E+01	0.67761E+01	0.53888E+00	0.60934E+00	0.16411E+01	0.30455E+01	0.60659E+00	0.62137E+00	0.11531E+01
0.13104E+01	0.18826E+01	0.70866E+01	0.51527E+00	0.63038E+00	0.15863E+01	0.30787E+01	0.58984E+00	0.61336E+00	0.11904E+01
0.13809E+01	0.19049E+01	0.74349E+01	0.49113E+00	0.64969E+00	0.15392E+01	0.31340E+01	0.57713E+00	0.60617E+00	0.12342E+01
0.15597E+01	0.19358E+01	0.77962E+01	0.46843E+00	0.67645E+00	0.14783E+01	0.31559E+01	0.58501E+00	0.59660E+00	0.12734E+01
0.16139E+01	0.19642E+01	0.81561E+01	0.44770E+00	0.70105E+00	0.14264E+01	0.31861E+01	0.56875E+00	0.58787E+00	0.13131E+01
0.16736E+01	0.19881E+01	0.85473E+01	0.42721E+00	0.72175E+00	0.13856E+01	0.32432E+01	0.56287E+00	0.58081E+00	0.13596E+01
0.18036E+01	0.20090E+01	0.89595E+01	0.40755E+00	0.73985E+00	0.13516E+01	0.33165E+01	0.54734E+00	0.57470E+00	0.14103E+01
0.19337E+01	0.20379E+01	0.93761E+01	0.38949E+00	0.76487E+00	0.13074E+01	0.33667E+01	0.54161E+00	0.56661E+00	0.14548E+01
0.20042E+01	0.20641E+01	0.98319E+01	0.37139E+00	0.78756E+00	0.12697E+01	0.34188E+01	0.52678E+00	0.55804E+00	0.15063E+01
0.20746E+01	0.20852E+01	0.10322E+02	0.36376E+00	0.80584E+00	0.12409E+01	0.36070E+01	0.50953E+00	0.55376E+00	0.15654E+01
0.22372E+01	0.21108E+01	0.10812E+02	0.33773E+00	0.82801E+00	0.12077E+01	0.35760E+01	0.50514E+00	0.54704E+00	0.16198E+01
0.23565E+01	0.21373E+01	0.11369E+02	0.32118E+00	0.85096E+00	0.11751E+01	0.36588E+01	0.49304E+00	0.54026E+00	0.16821E+01
0.24432E+01	0.21603E+01	0.11951E+02	0.30554E+00	0.87087E+00	0.11483E+01	0.37582E+01	0.47758E+00	0.53451E+00	0.17494E+01
0.26004E+01	0.21833E+01	0.12577E+02	0.29033E+00	0.89070E+00	0.11226E+01	0.38666E+01	0.46818E+00	0.52888E+00	0.18216E+01
0.27575E+01	0.22078E+01	0.13263E+02	0.27552E+00	0.91201E+00	0.10965E+01	0.39798E+01	0.45752E+00	0.52301E+00	0.18983E+01
0.28985E+01	0.22304E+01	0.13902E+02	0.26097E+00	0.93158E+00	0.10734E+01	0.41133E+01	0.44430E+00	0.51771E+00	0.19838E+01
0.30611E+01	0.22516E+01	0.14781E+02	0.24737E+00	0.94094E+00	0.10627E+01	0.42555E+01	0.43281E+00	0.51284E+00	0.20731E+01
0.32201E+01	0.22713E+01	0.15627E+02	0.23517E+00	0.96700E+00	0.10341E+01	0.43973E+01	0.42259E+00	0.50839E+00	0.21618E+01
0.33754E+01	0.22890E+01	0.16312E+02	0.22385E+00	0.98233E+00	0.10180E+01	0.45476E+01	0.41127E+00	0.50446E+00	0.22536E+01
0.35272E+01	0.23058E+01	0.17125E+02	0.21323E+00	0.99688E+00	0.10031E+01	0.47046E+01	0.40046E+00	0.50078E+00	0.23486E+01
0.36681E+01	0.23212E+01	0.17961E+02	0.20330E+00	0.10102E+01	0.98989E+00	0.48691E+01	0.38937E+00	0.49746E+00	0.24469E+01
0.38198E+01	0.23365E+01	0.18870E+02	0.19342E+00	0.10235E+01	0.97707E+00	0.50617E+01	0.37802E+00	0.49420E+00	0.25551E+01
0.39716E+01	0.23607E+01	0.19889E+02	0.18416E+00	0.10368E+01	0.96647E+00	0.52420E+01	0.36699E+00	0.49122E+00	0.26676E+01
0.41179E+01	0.23640E+01	0.20833E+02	0.17627E+00	0.10473E+01	0.95485E+00	0.54478E+01	0.35568E+00	0.48845E+00	0.27068E+01
0.42534E+01	0.23764E+01	0.21885E+02	0.16885E+00	0.10600E+01	0.94616E+00	0.56648E+01	0.34410E+00	0.48580E+00	0.28182E+01
0.43889E+01	0.23880E+01	0.23006E+02	0.15872E+00	0.10681E+01	0.93687E+00	0.58880E+01	0.33261E+00	0.48364E+00	0.30465E+01
0.45190E+01	0.23985E+01	0.24189E+02	0.15006E+00	0.10772E+01	0.92837E+00	0.61409E+01	0.32090E+00	0.48143E+00	0.31892E+01
0.46437E+01	0.24082E+01	0.25462E+02	0.14347E+00	0.10856E+01	0.92118E+00	0.64209E+01	0.30916E+00	0.47949E+00	0.33422E+01
0.47575E+01	0.24167E+01	0.26788E+02	0.13631E+00	0.10929E+01	0.91498E+00	0.67125E+01	0.29732E+00	0.47780E+00	0.35052E+01
0.48550E+01	0.24244E+01	0.28288E+02	0.12917E+00	0.10996E+01	0.90943E+00	0.70403E+01	0.28468E+00	0.47628E+00	0.36872E+01
0.49309E+01	0.24305E+01	0.29832E+02	0.12240E+00	0.11040E+01	0.90508E+00	0.73943E+01	0.27180E+00	0.47500E+00	0.38814E+01
0.49851E+01	0.24351E+01	0.31471E+02	0.11603E+00	0.11089E+01	0.90183E+00	0.77726E+01	0.25906E+00	0.47419E+00	0.40869E+01
0.50068E+01	0.24378E+01	0.33153E+02	0.11014E+00	0.11112E+01	0.89993E+00	0.81708E+01	0.24645E+00	0.47367E+00	0.43006E+01
0.50068E+01	0.24387E+01	0.36002E+02	0.10432E+00	0.11120E+01	0.89930E+00	0.86204E+01	0.23343E+00	0.47349E+00	0.45387E+01
0.49851E+01	0.24378E+01	0.37057E+02	0.98537E-01	0.11112E+01	0.89993E+00	0.91320E+01	0.22001E+00	0.47367E+00	0.48070E+01
0.49689E+01	0.24370E+01	0.39147E+02	0.93276E-01	0.11105E+01	0.90049E+00	0.96540E+01	0.20792E+00	0.47382E+00	0.50798E+01
0.49472E+01	0.24357E+01	0.41067E+02	0.88915E-01	0.11094E+01	0.90141E+00	0.10138E+02	0.19777E+00	0.47407E+00	0.53317E+01
0.49418E+01	0.24351E+01	0.42662E+02	0.85601E-01	0.11089E+01	0.90183E+00	0.10536E+02	0.19027E+00	0.47418E+00	0.55402E+01
0.49309E+01	0.24342E+01	0.44298E+02	0.82434E-01	0.11081E+01	0.90246E+00	0.10948E+02	0.18306E+00	0.47437E+00	0.57545E+01
0.49418E+01	0.24343E+01	0.46233E+02	0.78980E-01	0.11082E+01	0.90239E+00	0.11426E+02	0.17557E+00	0.47435E+00	0.60060E+01
0.49634E+01	0.24353E+01	0.48189E+02	0.75774E-01	0.11090E+01	0.90169E+00	0.11900E+02	0.16882E+00	0.47415E+00	0.62574E+01
0.50068E+01	0.24377E+01	0.50343E+02	0.72532E-01	0.11111E+01	0.90000E+00	0.12408E+02	0.16230E+00	0.47368E+00	0.65307E+01
0.54827E+01	0.24414E+01	0.52725E+02	0.69266E-01	0.11143E+01	0.89741E+00	0.12896E+02	0.15613E+00	0.47287E+00	0.68273E+01

TABLE II
DIMENSIONLESS QUANTITIES COMPUTED FROM FREESE-TRACEY DATA FOR AN ELLIPTICAL CRACK IN A TENSILE SPECIMEN

MATCHING FORMULAE

The following L and M formulae are selected from the many that were devised to match and smooth the L* and M data tabulated in Table II and shown in Figures 3 through 5.

With $F = Y(1+\Delta)$ for no pressure on crack faces,

$$L\,(\equiv Y\sqrt{\pi\rho}/K) = \frac{1}{1.29}\ln\frac{1.46}{\Delta+0.12}\ ;\ 0\le\Delta\le 1.11$$

$$= \frac{1}{1.29}\ln\frac{1.46}{S_m/Y-0.88} \qquad \text{when } F=Y(1+\Delta)$$

$$M\,(\equiv L\sqrt{x/\rho} \equiv Y\sqrt{\pi x}/K) = L\{\sinh[(8/3)\,\Delta]\,/2\}^{1/2}$$

$$= L\{\sinh[(8/3)\,(S_m/Y-1)]\,/2\}^{1/2}$$

L maximum is 2, and goes precipitately to effectively zero at

$\Delta \approx 1.11$, $0\le\Delta\le 1.11$

x/ρ *maximum is* 5, $0\le x/\rho\le 5$

S_m/Y *maximum is* $\approx 2.11Y$

---

* Considering the validity of data, etc., we actually use the formula for L to $\Delta = 1.11 = 10/9$, where, in fact L seems to sharply drop to zero; to approximately see this drop, multiply the L formula by $R=[1-(8\Delta/9)^{20}]^{.09}$. The Tables for L vs. Δ of the First Report may be used in place of the above L vs. Δ formula if the Δ's are multiplied by 3/4; see L vs Δ, p. 17.

If there is plane strain pressure, P, on the crack faces[13], $S_m = Y(1+\Delta)-P$.

The data is not precise below $\Delta = 0.25$, say, a caution, especially for those who use the data directly rather than through the formulae.

BRITTLE (NIL-DUCTILITY) TENSILE FRACTURE STRESS, EFFECTIVE RADIUS, YIELD STRENGTH

FRACTURE STRESS

If the tensile test temperature of a structural metal is lowered sufficiently the metal is found to break with little or no ductility. This stress is our fracture stress, F, if there has been slight straining, but not necessarily if the temperature is so low that there is no strain for there is evidence in at least some cases, that a completely undeformed specimen requires a higher stress for fracture than a slightly deformed one. In our case the greatest stress lies on the border of deformed material beyond the front of the crack. See Figure 6, where, assuming uniform yielding, F is about 60 ksi and high strain rate takes the place of low temperature.

F is of course, a macroscopic brittle, essentially nil-ductility tensile fracture stress, not the theoretical fracture stress of a homogeneous flawless material; the theoretical stress is presumably reduced to it by heterogeneity, flaws or inclusions.

For our conception of fracture stress see Fig. 7.

In the next section on use of the finite element data, we assume that for certain ranges of data that a linear fracture stress law may be used, i.e., $Y = (1 + \beta)Y + f$, where β and f are constants.

For the high strength steels with which he was familiar, the author observed, or inferred, that for tests at low to moderate temperatures covering practical ranges of brittle failure, that when the temperature of the tests alone was varied $F = f$, a constant*, and that when the tempering temperature of the test specimens alone was varied $F = Y + f$, i.e., the fracture stress was a constant amount above the yield strength, Y. These relations he generalized into a linear fracture stress "law" which he assumed suitable for the range of stress involved in the K_{Ic} determinations of ρ and F, i.e.,

$$F = (1 + \beta)\ Y + f$$

*Accordingly the writer observed that failure in guns occurred when the yield strength was raised by low temperature operation so that the concentrated yield strength equalled F, the fracture strength of the material of which they were made. (See Discussion)

Thus $\beta = -1$ for the varied test temperature tests above and $\beta = 0$ for the varied tempering temperature tests, above.

RADIUS

In the usual small deformation elastic solution corresponding to a flat elliptical notch in a tension field, the tip radius increases, in proportion to the load, depending on the modulus of elasticity, E; this is likewise the case for the non-cyclic loading elastic-plastic solution except that the proportion depends on the amount of yielding and thus on the yield strength and, to a more limited extent, on the work hardening modulus. The point here is that there is a unique radius for each load; the metallurgically dependent radii we have postulated do not exist for that fixed geometry.

But our deductions of radii, based on the curve fitting methods described in the next section are evidence that a change does take place at the very highly stressed tip, that we get radii other than above.

And, Taggart[13], fitting a parabola to the deflection of crack boundaries near the tip, found an increase in ρ with K, an increase to K_{Ic} load. The increase was not the same for different materials, as it would be if the crack tip radius increased uniquely with load for a given Y (and work hardening modulus, if large).

Thus, although F varies with Y, it is assumed in the analysis for ρ below, that ρ remains the same in any two ordinary test conditions for K_{Ic} unless the fracture shows a change such as, e.g., the appearance of cleavage fracture in the one test but not the other.

Theoretically, if not practically, according to the definitions of L and M, x the distance to the point of maximum stress along the crack axis could have been chosen instead of ρ as one of our crack characterization parameters.

YIELD STRENGTH

Perhaps this is as good a place as any to point out that a likely source of error is the use of conventional determinations of yield strength in our formulae. Our yield strength should be that of completely yielded material such as that determined by cyclic tests, even if the yielding is small. The conventional determinations are generally too high[16-18]; a particularly bad case is that of mild steel in which even the lower yield point represents non-uniform yielding, where the first yield is that of a slip band at an enormous rate of strain [(specimen length/slip band width) x nominal strain rate]. It is arguable that the endurance limit stress is the proper one; taking the yield strength to be half the tensile strength may be acceptable in some cases.

The fracture stress may be little above the apparent yield strength, but substantially above the actual yield strength.

USE OF THE FINITE ELEMENT DATA

MODE I STANDARD TEST K_{Ic} DATA

The object here is to determine F and ρ from K_{Ic} data obtained with pressure free crack faces. If only L (= $Y\sqrt{\pi\rho}/K_{Ic}$) is known for two or more cases, L must be supplemented by other information such as an appropriate fracture law, here taken to be $F = (1 + \beta)\ Y + f$, and assumptions supported by metallurgy and fractography of constancy of ρ and F in the range of data used in the determination.

Examples will be found in the First Report from which we have drawn Fig. 8. From this we note how well F and ρ determinations correspond to the experimental data as well as the effect of Sulfur level on the radius. Four cases are cited here, defined by what is used and constant (C ≡ constant) in the range considered.

M with L

F and ρ can be determined from the equations for L and M if x can be measured or inferred, e.g., from ripples which might result from successive fracturing and opening to the crack tip, especially if the incipient fracture is just off the center line of the crack, x being the distance from the tip of the crack to the site of incipient fracture. x may be of the order of one to five thousandths of an inch.

Thus in M we would have an expression in which all quantities except F are known; thus M determines F. Insertion of this F into L is an expression for ρ. A hand held computer which is programmable is handy for this.

L, β = -1, C(ρ,F)

For $\beta = -1$, corresponding to constant F at different test temperatures, F = f, a constant though Y changes. (See Fig. 9). Assuming F and ρ are the same for two data points, Y, K_{Ic}, two simultaneous equations may be formed and solved for F and ρ since each insertion of a data point Y, K_{Ic} into the expression for L provides an equation. Obviously, different combinations of data points may be used to check a result.

L, β = 0, C(ρ,f)

For β = 0, corresponding to tests at different tempering temperatures, F = Y + f where f is a constant and Y changes. (See Fig. 8) Since we assume ρ = constant (subject to constancy of existence of the weakest kind of fracture, e.g., grain boundary fracture).

$$L \equiv Y\sqrt{\pi\rho}/K = \mathit{function}\,(F/Y)$$

we have for two data points:

$$Y_1\sqrt{\pi\rho}/K_1 = \mathit{function}(1+f/Y_1)$$

and

$$Y_2\sqrt{\pi\rho}/K_2 = \mathit{function}\ (1+f/Y_2)$$

These may be solved simultaneously to find f and ρ.

L, β, C (ρ, F) and L, C (ρ, f)

The scatter in experimentally determined values of K is often so pronounced that a curve fitting procedure using transparent overlay graphs and involving more K_{Ic}, Y values is recommended, as described in the First Report and repeated, in part, in Appendix I - Overlays. (See Figs. 10-12.)

It will be recognized by some that this overlay procedure can be done very readily on a computer; for example, following the procedure of K_{Ic} versus Y for various tempering temperatures of steel for which $\beta = 0$, plot ln $(1/\Delta L)$ versus ln $(1/\Delta)$ from the equation for L versus Δ, the overlay, and separately, plot the K_{Ic} versus Y data as ln K versus ln Y. Move the latter plot of points, along with its coordinates, parallel to the coordinates of the ln $(1/\Delta L)$ versus ln $(1/\Delta)$ plot until the points fit the curve of the latter plot. Then f, a constant, is that coordinate value of Y where the ln Y coordinate is crossed by the unit vertical coordinate of the overlay and, similarly, $f\sqrt{\pi\rho}$, a constant, is that coordinate value of K where the ln K coordinate is crossed by the unit horizontal coordinate of the overlay. Then F = Y + f where Y is any Y and* ρ is $(f\sqrt{\pi\rho})^2/\pi f^2$.

Generally, a master reusable ln ln plot of $[1/(\Delta-\beta)L]$ versus $[1/(\Delta-\beta)]$ is made on transparent ln ln paper as a bank of β constant curves; this overlay is placed over any particular plot of K, Y data on the same size of ln ln paper as the transparency and slid parallel to the coordinates to the β curve which best matches the data; this determines β and, simultaneously, f and ρ;

*From experience it is seldom worthwhile to allow for the elastic change in ρ as is done in the First Report.

f is that coordinate value of Y where the Y coordinate is crossed by the unit vertical coordinate of the overlay and $f\sqrt{\pi\rho}$ is that coordinate value of K where the K coordinate is crossed by the unit horizontal coordinate of the overlay.

HYDROSTATIC PRESSURE MODIFICATION OF K_{Ic}

K_{Ic} formulae obtained by energy methods are independent of hydrostatic pressure[1]. This particular consequence may be justified by the belief that there is always an infinite stress singularity at the tip of the crack.

Here, however, it is believed that for metallic materials of construction, at least, there is an effective crack tip radius at any load; that consequently all stresses are finite and reduced by the addition of hydrostatic pressure; that K_{Ic} failure will occur if the largest stress equals the tensile brittle fracture stress, F, of the material.

Thus we now consider how to modify K_{Ic} determinations to make them applicable to the case where there is uniform pressure on the crack surface, a pressure that might be applied by superimposing on the standard loading a hydrostatic pressure.

A plot of L vs. Δ for a crack in a distant field of uniform tension S* is a plot of $[(S/Y)(a/\rho)^{1/2}]^{-1}$ vs. Δ where if S/Y and a/ρ are known one finds Δ. The addition of a plane hydrostatic** pressure P does not change the yielded areas, their boundaries or the geometry; it only makes the size slightly and negligibly smaller. It does not affect the yield boundaries of the lobes of yielded regions at the tips of the crack; therefore Δ is not changed. P, however, is added (negatively) to every component of normal stress, including boundary loading stress, S, but we still think of the boundary loading stress (S - P) as made up of its two components since only S controls Δ; L in L vs. Δ does not contain P; it is still $[(S/Y)(a/\rho)^{1/2}]^{-1}$. Though Δ is unchanged it is used to determine S_m; if there is no P, we have $S_m = Y(1 + \Delta)$ but if there is an addition of hydrostatic pressure P, as described*** above, $S_m = Y(1 + \Delta) - P$.

Thus without P, $\Delta = S_m/Y - 1$ and with P, $\Delta = (S_m + P)/Y - 1$ although K is independent of P in $L = Y\sqrt{\pi\rho}/S\sqrt{\pi a} = Y\sqrt{\pi\rho}/K$.

---

*The Griffith case, but equivalent for an ideal crack to the case of uniaxial tension perpendicular to the crack.

**Obviously, the original loading could have been in the crack instead of applied externally in which case P (if P was the loading) would be in L instead of S. We choose the external case here because it is the case for which K_{Ic} measurements are made.

***According to the equilibrium equations, for a material where it undergoes a constant yielding stress , Y, Δ corresponds to an increase Δ Y over the magnitude of the principal stresses at the crack side of the boundary of the yielded region (lobe boundary) by the corresponding stresses located by following a principal shear stress trajectory, on the other side. Thus, the magnitude of a principal stress (Y - P) on the crack side becomes $(Y - P) + \Delta Y = Y(1 + \Delta) - P$ for a corresponding one on the other side as the difference in directions is Δ. This is the same, of course, as increasing the original S_m stress, $Y(1 + \Delta)$ by the hydrostatic stress -P.

Obviously, if $S_m = F$, a material constant, Δ is greater on the L vs. Δ plot with P than without P.

Thus, a knowledge of F and ρ found from a standard test specimen K_{Ic} can be used to determine what 'K_{Ic}' value should be used if there is known internal pressure P: $\Delta = (F + P)/Y - 1$, this determines L; then $K_{Icp} = Y\sqrt{\pi\rho}/L$, calling K_{Icp} the critical 'K_{Ic}' with pressure, a quantity larger than K_{Ic}.

With guns, $|P| = S$, so there is no external loading stress, only an internal pressure (S).

QUANTITATIVE RELATIONSHIP BETWEEN THE FINITE ELEMENT AND FIRST REPORT RESULTS

L versus Δ

A comparison of the data for the basic L versus Δ curve of the First Report and the present Freese-Tracey finite element data indicates to possibly 95% accuracy that for any specified value of L, and thus any combination of Y, K_{Ic} and ρ making up that value of L, in either source,

$$\Delta = (3/4)\Delta_1$$

where the subscript "1" stands for the First Report.*

* Thus the L vs Δ Tables of the First Report may be used to Δ cut-off if the tabulated Δ's are multiplied by 3/4.

Since, also

$$F = Y(1 + \Delta)$$

$$F_1 = Y_1(1 + \Delta_1)$$

we have

$$F/Y - 1 = (3/4)(F_1/Y_1 - 1)$$

where $$L = Y\sqrt{\pi\rho}/K_{Ic} = Y_1\sqrt{\pi\rho_1}/K_{Ic1}$$

In particular, if $Y = Y_1$, so that it is also necessary that

$$\sqrt{\rho}/K_{Ic} = \sqrt{\rho_1}/K_{Ic1},$$

$$F - Y = (3/4)(F_1 - Y)$$

which may be rewritten for different insight as

$$F = Y + (3/4)(F_1 - Y)$$

$$F = 3/4\ F_1 + Y/4$$

$$F = F_1 - (F_1 - Y)/4$$

$F = (1 + \beta)Y + f$ **vs.** Δ

Next, we note how the linear fracture stress laws compare, also using $F = Y(1+\Delta)$ and $F_1 = Y_1(1+\Delta_1)$.

Since we wish the consequence of a particular assigned value of β in either case, $\beta = \beta_1$; in designating β we are thus defining F in terms of Y and f:

$$F = (1+\beta)Y+f$$

$$F_1 = (1+\beta)Y_1+f_1$$

We note the result of elimination of β from these as well as two cases of special interest, $\beta = 0$ and $\beta = -1$.

<u>By elimination of β</u>

$$f/Y - f_1/Y_1 = (F/Y-1) - (F_1/Y_1-1)$$

whence, since $F = Y(1 + \Delta)$ and $F_1 = Y_1(1+\Delta_1)$,

$$f/Y - f_1/Y_1 = \Delta - \Delta_1$$

and thus if $Y = Y_1$,

$$f - f_1 = Y(\Delta - \Delta_1)$$

where we can substitute for the angles their expressions in L.

<u>For $\beta = 0$</u>, with $Y_1 = Y$:

$$F = Y + f,\ so\ F/Y - 1 = \Delta = f/Y$$

$$F_1 = Y + f_1,\ so\ F_1/Y_1 - 1 = \Delta_1 = f_1/Y$$

$$\Delta = (3/4)\,\Delta_1;\ \therefore\ f/Y = (3/4)\,(f_1/Y)$$

i.e.,

$$f = (3/4)\,f_1$$

We noted in <u>L vs. Δ</u> that $\Delta = (3/4)\Delta_1$ used here, was for equality of L's in the expressions for Δ vs. L.

Thus,

$$\rho = \rho_1$$

since we assume $Y = Y_1$ and $K_{Ic} = K_{Ic1}$ in the expression for L.

See Figure 11, the $\beta = 0$ overlay for the First Report, on which new axes have been added making it valid for the new finite element data $\Delta = (3/4)\Delta_1$; these axes are displaced downwards and to the left by ln (3/4) from the old ones; this follows from the fact that on ln ln paper the old coordinates are $1/\Delta_1 L$ vs $1/\Delta_1$ while the new ones are $1/[(3/4)\Delta_1 L]$ *vs.* $1/(3/4)\Delta_1$, i.e., on ln ln paper we have $\ln(1/\Delta_1 L) - \ln(3/4)$ *vs.* $\ln 1/\Delta_1 - \ln(3/4)$.

<u>For $\beta = -1$</u> the strength law gives

$$F = f$$

$$F_1 = f_1$$

From this because $\Delta = (3/4)\ \Delta_1$ we have for $Y = Y_1$,

$$F/Y - 1 = (3/4)(F_1/Y - 1)$$

i.e.,

$$F = (3/4)F_1 + Y/4$$

as was expressed above under <u>L vs. Δ</u>, although the strength law is designed to make F independent of change in Y for $\beta = -1$. The consequences are discussed below.

Using the First Report data, if one found F and ρ for $\beta = -1$ by precisely matching experimental observations of K_{Ic} and Y, one could not get a precise match for F and ρ using the new data for $\beta = -1$; one would have to change β to get a match; in this case, $\beta = -1$, would change to $\beta = -3/4$:

$$\frac{1}{\Delta-\beta} \rightarrow \frac{1}{(3/4)\Delta_1+3/4} = \frac{1}{3/4\,(\Delta_1+1)}\ .$$

where the second expression is, of course $\Delta + 3/4$. On ln paper the 3/4 is simply a translation movement; no change in shape takes place. But this is not the desired match for $\beta = -1$ for the finite element solution if the match was made for $\beta = -1$ for the First Report.

Thus, believing in the utility of the $\beta = -1$, i.e., $F = f$, independent of Y result for tests at various test temperatures, we conclude that there was not an exact correlation for $\beta = -1$ tests in the First Report, though a useful one.

What we find is that a very satisfactory correlation, a satisfactory match for the useful range of data, exists between the $\beta = -1$ overlays for the new and old data, that is the overlays whose axes intercepts on the ln ln plot of K_{Ic} vs. Y determine F and ρ. For the First Report the overlay is a ln ln plot of $1/[(\Delta_1+1)L]$ *vs.* $1/(\Delta_1+1)$; for the new work it is $1/[(0.75\Delta_1+1)L]$ *vs.* $1/(0.75\Delta_1+1)$, since $\Delta = 0.75\Delta_1$. These two plots match quite well if the horizontal axis of the latter is displaced to ln 0.935 downwards and the vertical axis is displaced leftwards to ln 0.855, of the original First Report axis.

These new axes are shown in Figure 12.

The intercepts determining F and ρ are displaced the same amount.

Thus,

$$F = 0.855F_1$$

and

$$F\sqrt{\pi\rho} = 0.935\ F_1\sqrt{\pi\rho_1}$$

i.e.,

$$0.855F_1\sqrt{\pi\rho} = 0.935F_1\sqrt{\pi\rho_1}$$

$$\rho = 1.196\ \rho_1$$

DISCUSSION AND CONCLUSIONS

Before taking the Freese - Tracey data as definitive and comparing it with those of the First Report, it should be pointed out that the maximum stress reported in the First Report was not on the center[2] line of the crack but just to one side of it (except for initial yielding) while the maximum stress reported by Freese - Tracey was on the center line; the grid used was too coarse to make such a distinction. It should also be pointed out that Freese - Tracey data is scattered for small degrees of yielding, and equal stress loading along and perpendicular to the crack was used in the First Report and simple tension in the Freese - Tracey case (a difference possibly of consequence if yielding is relatively extensive). The shear case was solved (not published) by the method of the First Report and showed no concentration of stress; a result which seems to conform with experiment, thus, the method is of interest in considering the above points.

Except for a sort of scaling factor, correlations of K_{Ic}, Y data to find F and ρ by Freese - Tracey and the First Report are practically equivalent. Thus, to use the excellent correlations in the examples of the First Report, one only need to change for $\beta = 0$, $f = (3/4)f_1$, $\rho = \rho_1$ and for $\beta = -1$, $F = .855\ F_1$, $\rho = 1.196\ \rho_1$ where the "$_1$" refers to the First Report results.

However, there is a very important difference in the two sets of data: there is an upper limit to $\measuredangle$ found by the finite element approach, $\measuredangle = 1.125$, corresponding to a limiting distance of yielding ahead of the crack of $x/\rho = 5$. This angle means that the greatest stress there can be in this basic crack problem is

$(1 + \Delta)\ Y = 2.11Y$; this is less than the $(1 + \pi/2)Y$ of the slip line theory for the straight line crack and much less than might be expected from the First Report.

What this means in practice is that if the fracture stress of the material, F, is greater than 2.11Y, no K_{Ic} crack failure will occur.

This kind of limitation, a characterization which seems very important in practice, is even stronger than was anticipated by former analyses, if not by experiment or practice. As an example, for some pieces of ordnance equipment, the fracture stress F of the material of which it was made was flat over the temperature range of its possible employment; when the equipment was used (i.e., loaded) at its normal temperature of operation there was no brittle K_{Ic} failure, but when the equipment was loaded at a reduced temperature, Y became sufficiently great for brittle K_{Ic} failure to occur. The factor of concentration was F/Y; i.e., $(1 + \Delta)$ See Figure 9.

Obviously, the fracture stress* of the material, F, should be found by separate experiment if possible. Also, as far as is known, the two physical quantities F and ρ are metallurgically independent. If this is so, the metallurgist has two fabrication

*There are certain metals in certain states for which Griffith's surface energy density seems to hold using his formulation. It is doubted that K failure values for structural metals have been appropriately studied for comparison or otherwise in the state in which they are macroscopically brittle, i.e., well below the transition temperature, a state usually avoided in practice, but having some uses.

options for attaining a suitable K_k. There is evidence in the First Report that ρ is dependent upon structure and sulfur (see the First Report). If F, ρ (possibly machined in) and Y are specified K can be found from $L = f(\Delta)$, i.e.,

$$Y\sqrt{\pi\rho}/K = f(F/Y-1).$$

In the case of the example above, the brittle fracture stress could be inferred since a temperature low enough for brittle fracture to occur in a simple tension test could be attained using available coolants such as liquid nitrogen. This is the case for some other materials such as mild steel and tungsten (see Figure 6), which illustrates stress-strain curves with their fracture envelopes. Many such curves were drawn to represent the results of many tests on steel at this laboratory. The "nil ductility" brittle fracture stress is considered to be **almost** nil ductility since it is possible that a test under hydrostatic tension on virgin material would yield a higher value corresponding to a microstructure unaltered by plastic straining; this, if true, is of no concern here because the present model presumes yielding and fracture at the boundary of plasticity.

Other attempts to determine fracture stress have been inconclusive because they are unfinished. They are:

- Attempt to use certain notch geometries in tension tests with partial yielding.

- Attempt to put uniform exterior tension loading on a plate containing a hole; the reason for using this arrangement is that with it there is a maximum stress which occurs at the boundary of the plastic region (which extends outward from the bore) and which for sufficient load may cause rupture. Since this experiment was difficult to carry out, the same thing was at least partially achieved during many trials by pressing a ball about a quarter of an inch in diameter onto the top side of approximately one inch square plates supported circularly near their outer edges and pierced with a 0.01* inch diameter hole. The behavior was observed on a television screen which picked up the view of a microscope focussed on the bottom side.

- Attempt to use the Fyfe exploding wire technique at the University of Washington through contracts. Here a coated wire in the bore of a cylinder of an inch or less in diameter is exploded by the controlled electrical discharge of electricity stored in a condenser bank. It was easy and **very** inexpensive to

*Once, the 0.01 inch hole expanded to 3/16 inch diameter before failure, a strain of 1275%.

cause controlled subsurface (to the hole) rupture; i.e., complete or incomplete rupture. Thus, an effect of anisotropy could be seen. This was better, for purposes of this report than plate-slap experiments partly because rupture was not preceded by an enormous deforming compression of the material being tested before a tension wave caused rupture. There was a very important quantitative question, however, about the magnitude of the pressure generated, as well as a question of whether important high strength materials could be broken. Unfortunately, these questions could not be answered before the work was terminated.

In the above cases a fracture stress is determined from a multi-directional stress system resembling that of the loaded crack. Thus the necessity of a failure concept for use of a uniaxially determined fracture stress is largely avoided.

In the case of the unpressurized crack or notch deformed in plane strain, there is a stress $Y + Y\Delta$ acting perpendicularly to the crack axis which we have associated with the brittle uniaxial tension test, and a stress $Y\Delta$ along the axis. Fracture openings (preventing crack growth) have occurred across this lesser stress, the material involved being much weaker in its direction than in that of the major stress.

In summary this study relies for fracture on the macroscopic stress found to give almost nil ductility in the tension test. It is important to note that creep or other rate effects may occur at the tip of the crack and, since the region to the point, x, of largest stress is so very small and has yielded, that the fracture stress is environmentally sensitive; thus progressive cracking is to be expected depending on contaminants and the diffusion rate of hydrogen in the yielded region. The theoretical fracture stress used by Griffith is estimated to be reached microscopically at internal flaws but strengths and failures at these individual flaws are not representative of the macroscopic crack strength where failure covers many grains. The situation is somewhat analogous to that where it may be desired to determine the tensile fracture strength of a structural component, a plate pierced by many holes or irregularities, a case where one measures the strength by dividing the breaking load of the plate by its nominal cross-sectional area, independently of phenomena occurring at individual holes.

Here as the load is increased there is a gentle transition of the largest stress S_m from being proportional to the load to being less responsive to it as the point of largest stress, x, moves increasingly sub-surface and finally not responsive to the load at all when the stress reaches 2.11Y and $x = 5\rho$. If S_m does reach $2.11Y < F$, a marked transition occurs since from this point on only ductile separation can occur; the crack opens up and the yield region changes. If S_m does equal F after the yield point is reached brittle fracture occurs. The failure of a Charpy Bar is somewhat similar: above the transition temperature corresponding to complete yielding below the notch the separation surfaces open into a wide V of fixed angle which continues until final separation occurs; below the transition temperature the separation surfaces remain almost closed during fracture.

According to the model used in this study, plastic lobes at the crack tip along with their shear stress trajectories give rise to the maximum stress and they move as cracking proceeds. Work is done on their creation and some of it is given back in movement; this loss must be supplied by the loading. Our old attempts to calculate these lobe generating energies and losses were not completed to our satisfaction; questions involving inelastic behavior remain. For a finite element treatment see reference 5.

An addition of hydrostatic pressure reduces all stresses and thus the proximity of breakage on the stress approach to K_{Ic} failure although the formulae for K_{Ic}, which may be derived from energy considerations, are independent of this effect; it is the value for K_{Ic} that differs with different materials; and in view of the stress reducing effect of hydrostatic pressure, the value found from standard tests using specimens with stress free crack faces are not applicable to pressurized crack faces. We show how to modify the standard values to K_{kp} values which are applicable.

Finally, let us examine Griffith's "The Theory of Rupture" to see if his approach, which is commonly characterized as an energy approach, is inconsistent with the author's approach.

Considering the lack of appropriate scientific knowledge to do otherwise, Griffith confined himself to brittle solids obeying Hooke's Law which might contain one or more cracks. The stresses in the solids he computed from ordinary elasticity theory including the stress to cause rupture. The latter stress was taken to be comparable to the intrinsic internal pressure of the solid (meaning atomic vibration pressure sufficient to cause vaporization) corresponding to a strain energy density for rupture comparable to the total heat of vaporization. Rupture would represent an enormous temperature rise in the material if the elastic strain energy did not go into surface energy as in the extremely large surfaces associated with disintegration (e.g., breakage of very thin new glass rods) or, locally, not concentrated at the end of a crack and, therefore, go into new surface if the crack were to lengthen. In fact, his well-known formula represented a crack stressed so that if it were to lengthen a bit (rupture) equilibrium would be maintained; i.e., its new surface energy would come from the strain energy of the solid and potential energy of the loads so that the total energy would be unchanged. Surface energy density being a constant, shorter cracks would be stable and longer ones unstable, for a fixed loading, since the stress is greater for longer cracks.

Thus, we observe that Griffith relied on the ideal theoretical rupture stress for both cracked and uncracked solids, but, leaning heavily on experiments on glass, assumed that often cracks were formed historically which weakened a solid and made its tensile strength less but computable for simple geometries from the ideal rupture stress or its corresponding surface energy density and he derived his failure condition from an energy balance.

Thus Griffith would seem to have neatly connected both stress and energy approaches. But the crucial thing is would he have used a different surface energy density value than he contemplated if he had thought of our dodge* of making the Griffith derivation trivial by employing internal[15] rather than with external loading (and so avoided the error in his first paper)? We prefer to think he would have done so and so agreed with our different K_{Ic} value for internal than external loading.

*Making the pressure cancel the exterior loading so that all the loading is inside the crack makes the derivation of the Griffith formula extremely simple since the energy due to the crack is simply the work done by the pressure in creating volume change inside the crack as a result of the pressure (see Appendix II).

ACKNOWLEDGMENTS

To Colin Freese for his review and supply of data in an appropriate form and to Albert Kobayashi and Donald Oplinger for their reviews.

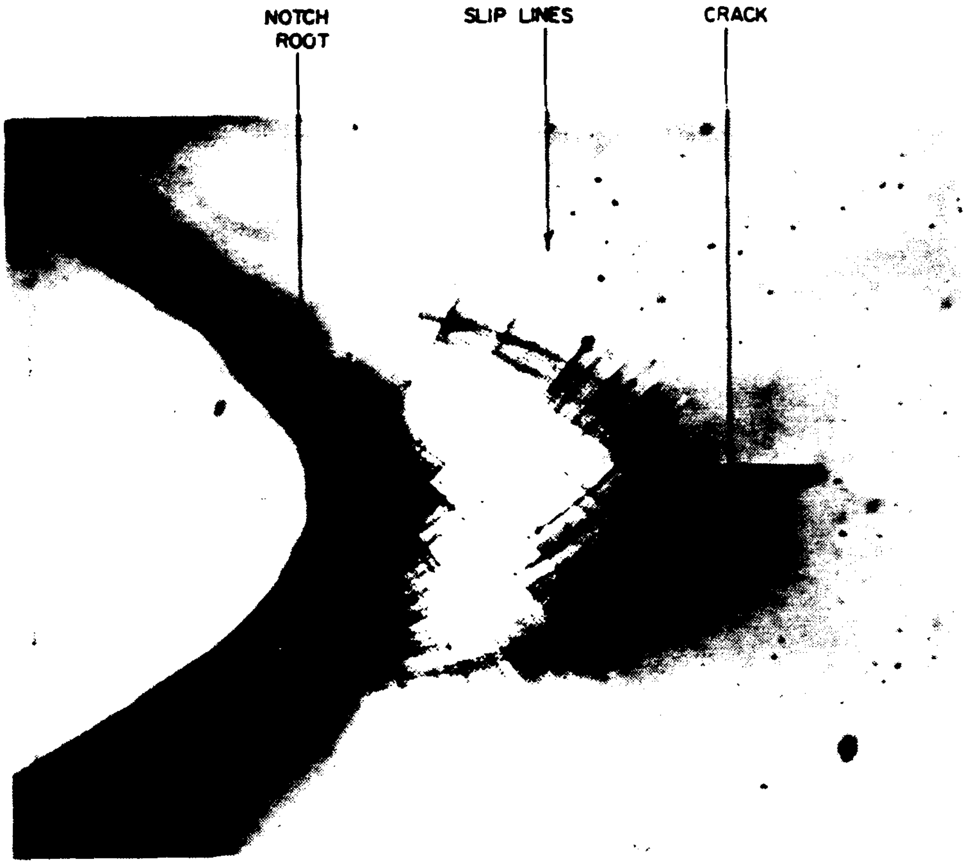

Transverse View of Mid-Thickness Slice Showing Fracture Origin At Elastic-Plastic Boundary and Slip Lines. ρ = 0.005 In. 350x.

FIGURE 1

PARABOLIC CRACK
Partial Plasticity - General Features

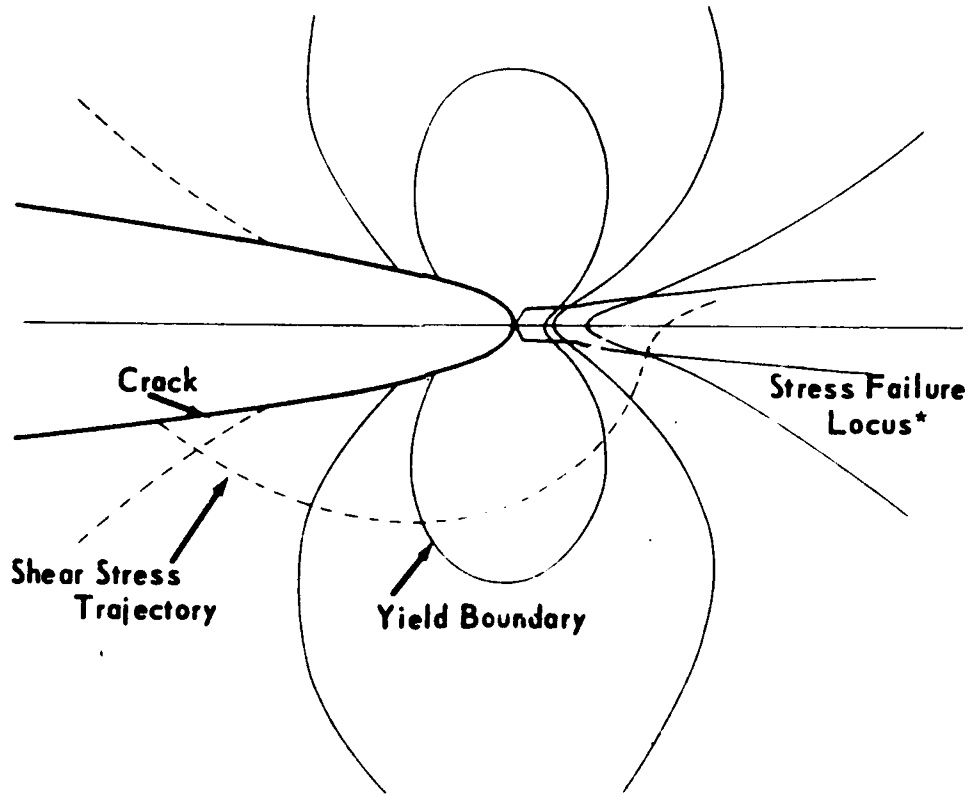

*Max Stress occurs at interseciion of this locus and yield boundary.

FIGURE 2

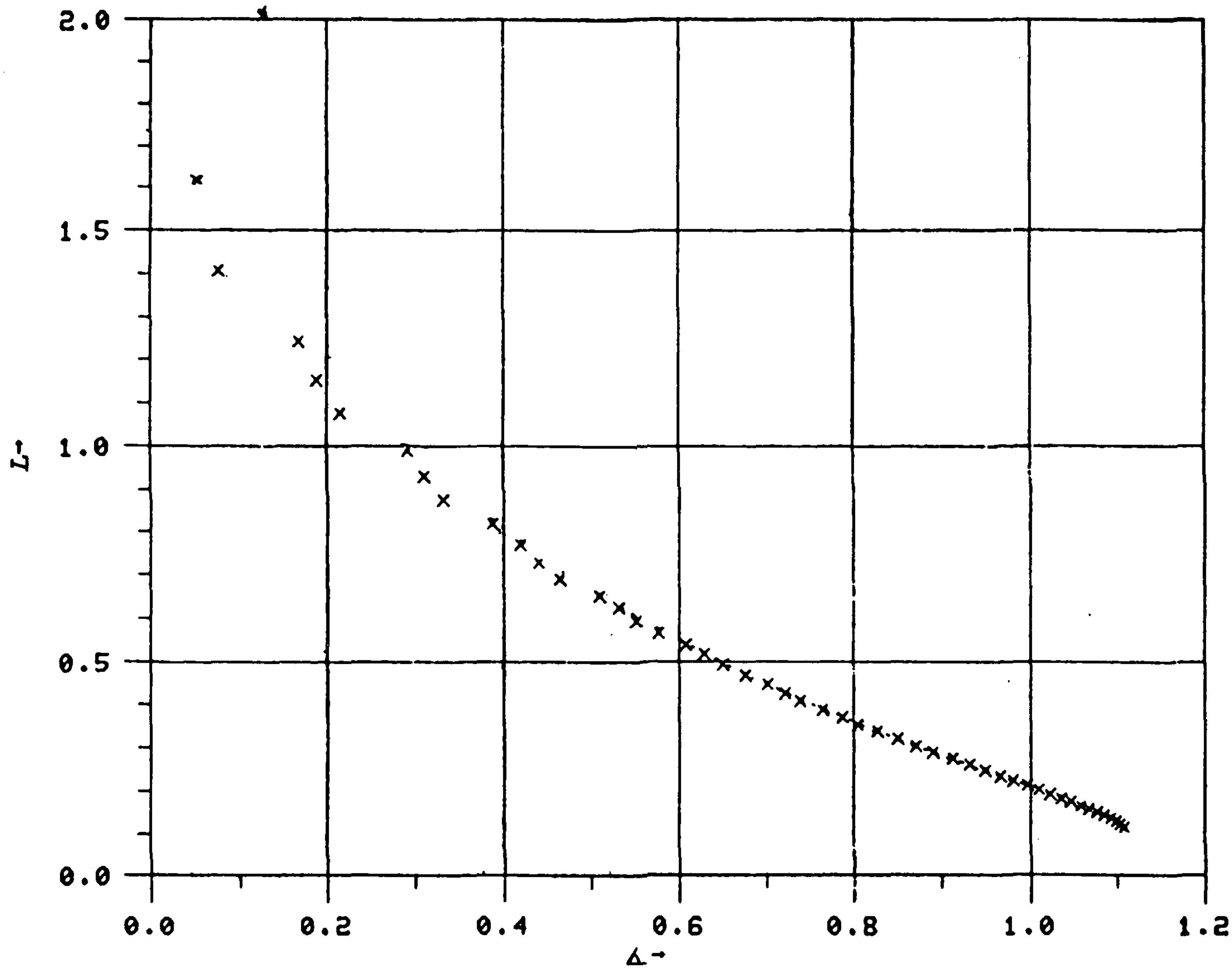

FIGURE 3. L vs. Δ. Freese-Tracey Data

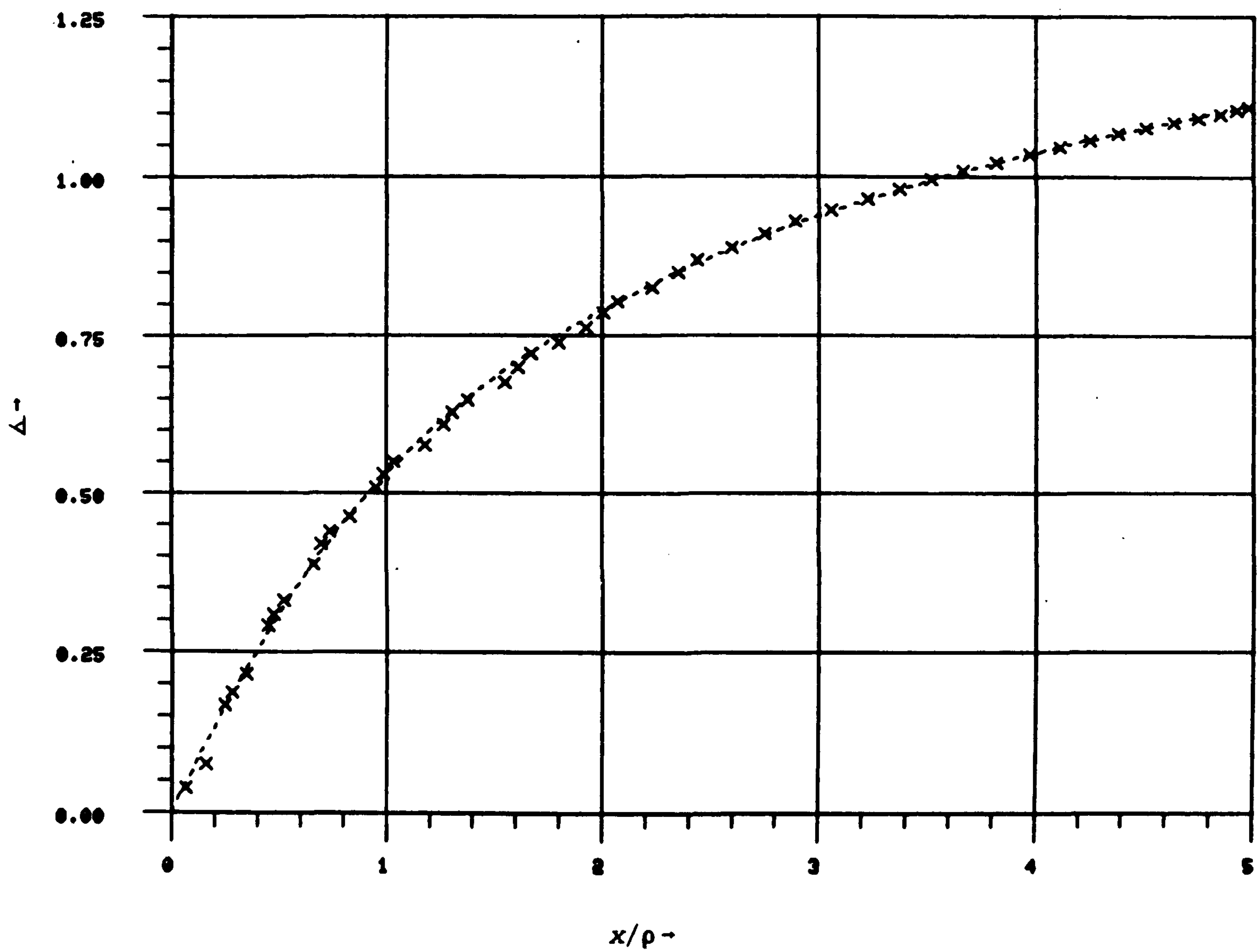

FIGURE 4. Δ *vs.* x/ρ. Freese-Tracey Data

14 March 1985

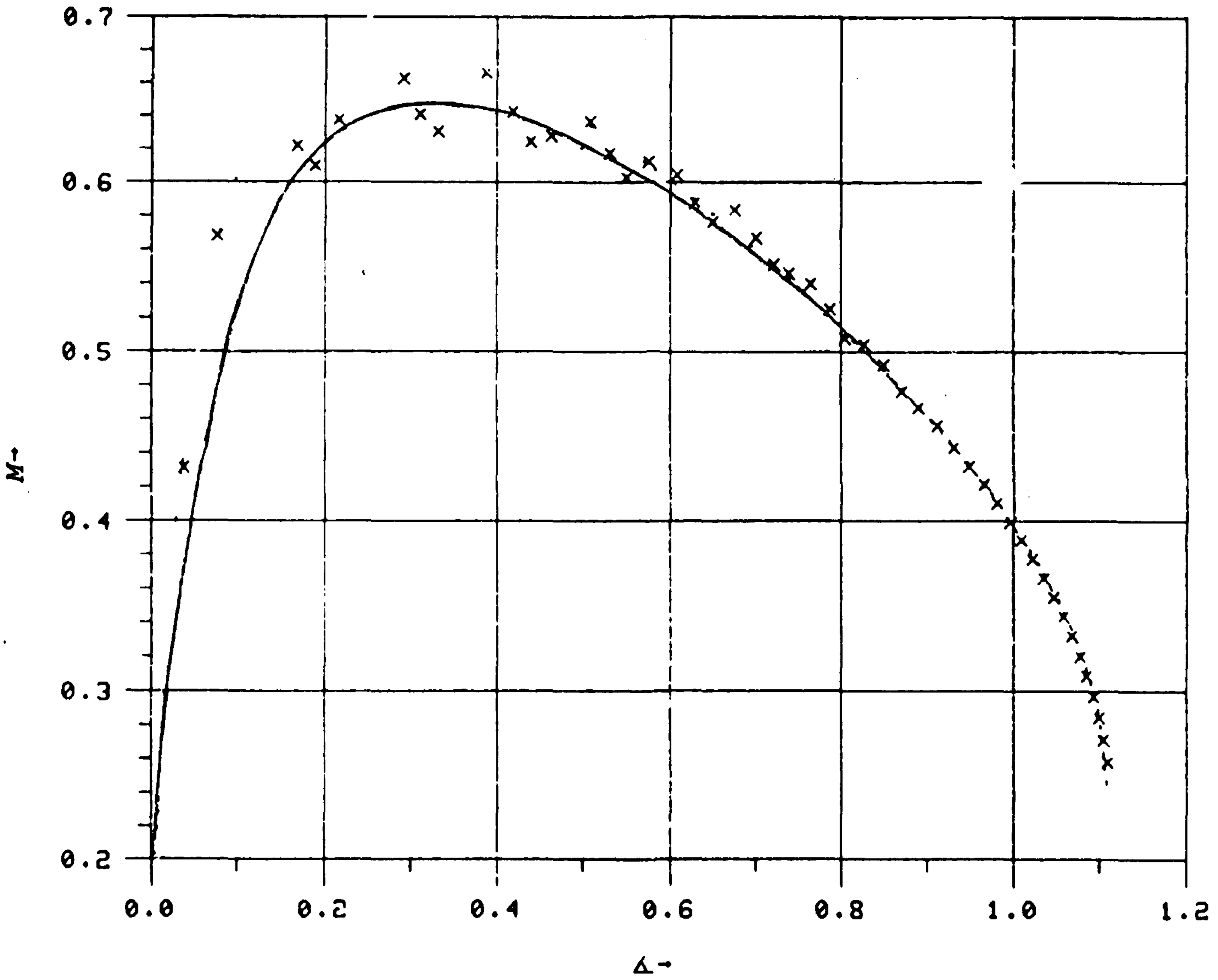

FIGURE 5. M vs. Δ with Matching Curve
Freese-Tracey Data

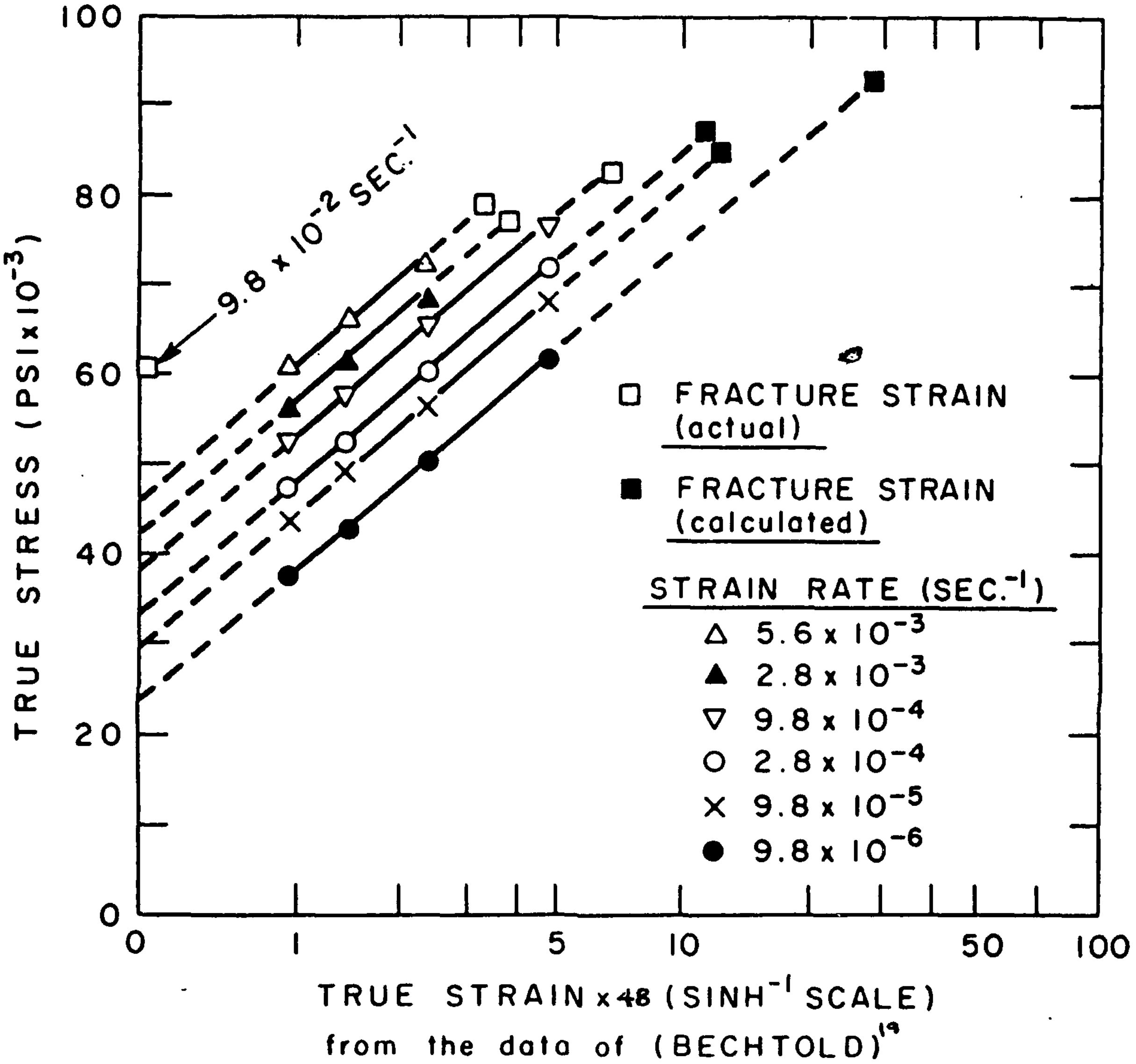

True stress – true strain curves for annealed tungsten. Test temp.=523°K

FIGURE 6

A FRACTURE MODEL: FRACTURE STRESS S_f

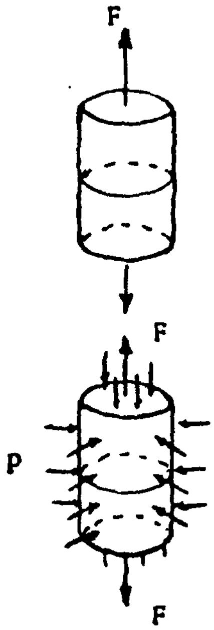

AMBIENT PRESSURE: $p = 0$

SET ONE BLOCK ON ANOTHER. LOAD, F.

FRACTURE (LOAD AND) STRESS? $S_f = 0$.

AMBIENT PRESSURE: $p >> Y$

BLOCKS IN SHEATH. LET $F/A > Y$.

PLASTIC ELONGATION? YES.

STRESS F/A AT FRACTURE? p.

FRACTURE STRESS? $S_f = 0$.

NOTE: The mating surfaces need not be flat

a) FRACTURE STRESS = MAXIMUM STRESS ACROSS WEAKEST PLANE, INCLUDING HYDROSTATIC STRESS; SAME FOR NOTCHES.

b) LATERAL FRACTURE STRESS MAY BE LARGE.

(R. BEEUWKES JR.)

19-066-1159/AMC-67

MEANING OF FRACTURE STRESS

FIGURE 7

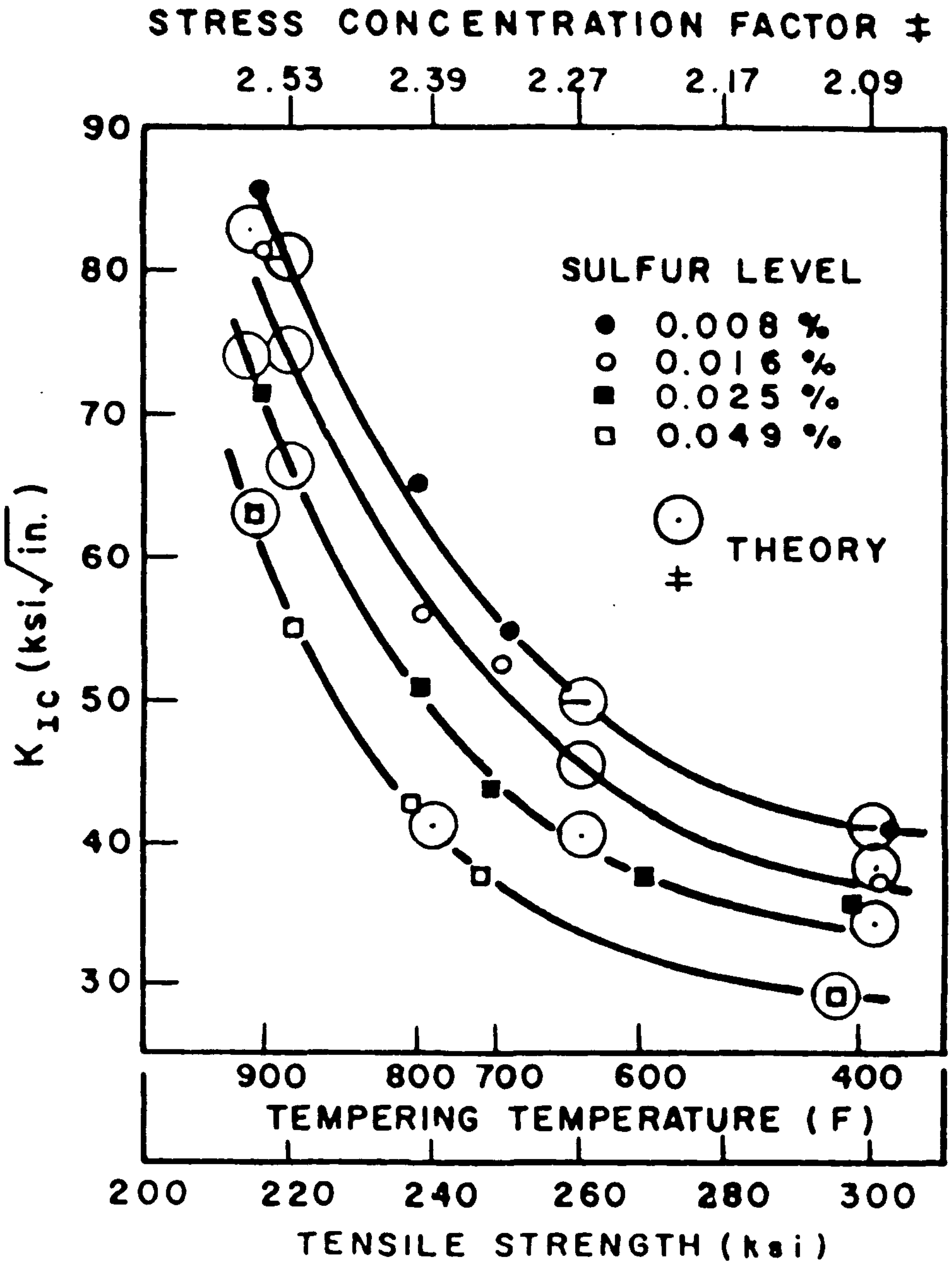

INFLUENCE OF SULFUR ON PLANE-STRAIN FRACTURE TOUGHNESS OF 0.45C Ni-Cr-Mo STEELS (Experiments: A. J. Birkle, R. P. Wei, and G. E. Pellissier, U. S. Steel Corp. Theory: R. Beeuwkes, Jr. - Fracture Stress = 285.5 + Tensile Strength; Radii x 10^4, in., = 9.28, 7.83, 6.33, 4.48 for 0.008, 0.016, 0.025, 0.049 respectively.)

FIGURE 8

BRITTLENESS: Stress Concentration k, to Cause Failure, $e = 0^+$
(R. B. Jr., Idealization)

Idealization

1. $|F - Y|_T$ is Independent of Strength Level

2. $|F|_{e,\dot{e}}$ = Constant

3. $F = s(e)$

4. Material ~ Independent of Time

5. K is from Plasticity Theory

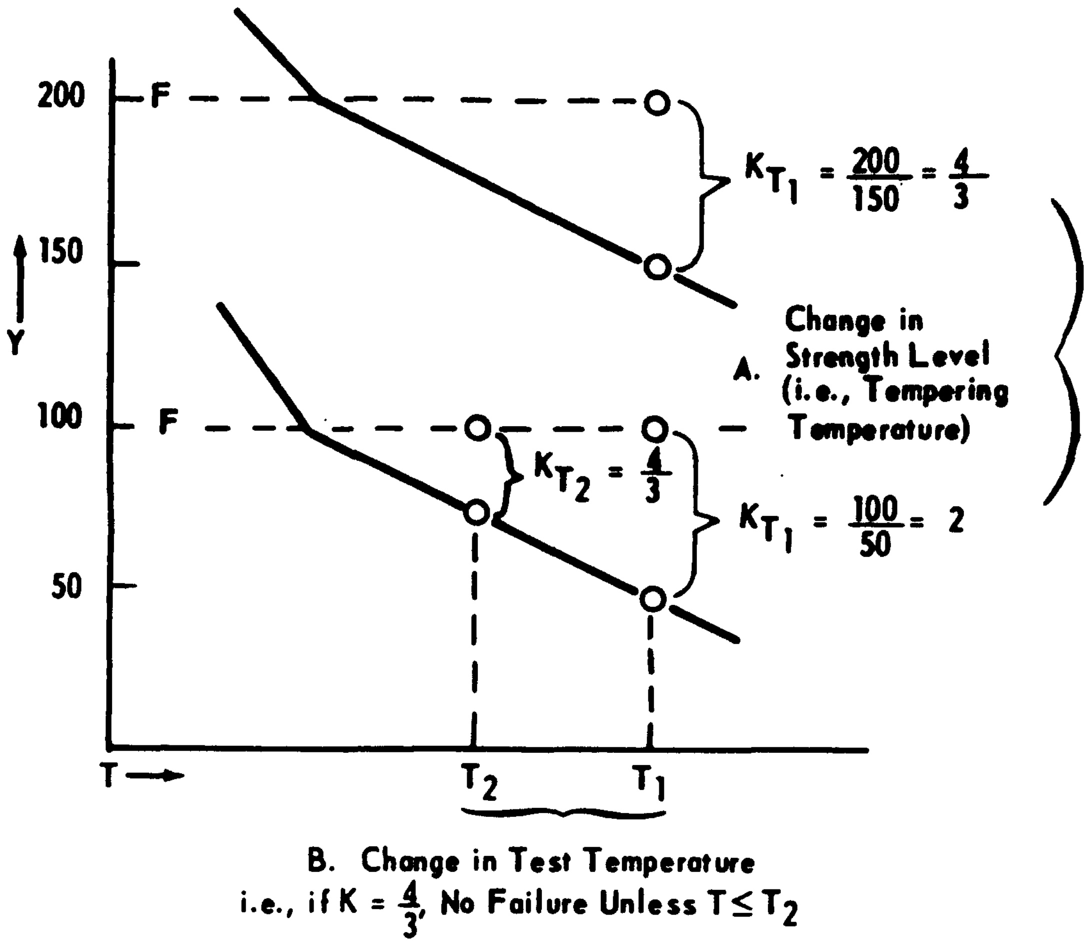

FIGURE 9

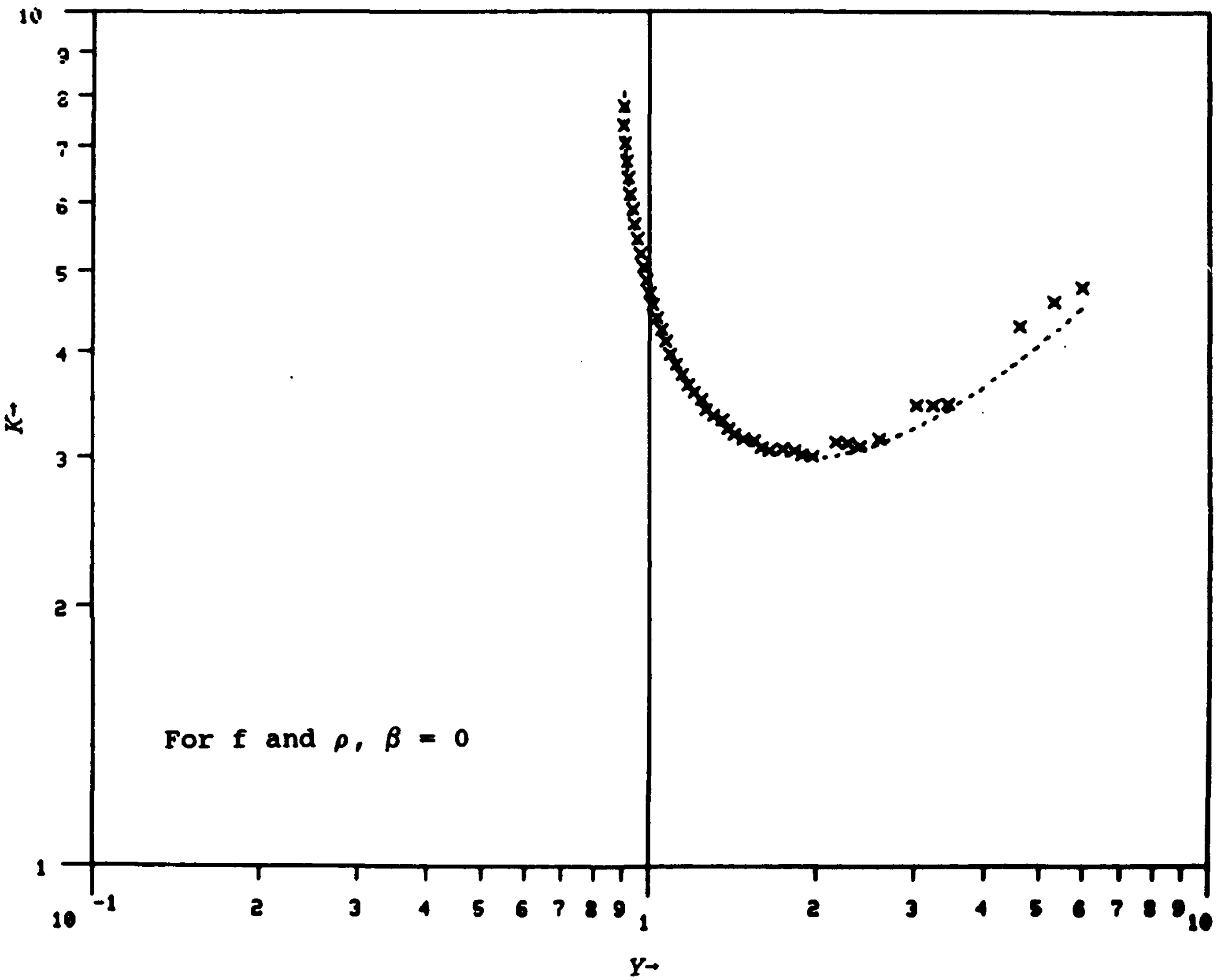

FIGURE 10. (1/ΔL) VS.(1/Δ) on ln ln paper, Freese-Tracey Data

f β = 022 March 1985

Constant f Overlay

Applicable where f(=F-Y) and ρ do not vary with Y(β=0).

1. Plot K vs Y data on single-cycle log-log paper (Keuffel and Esser No. 458-100, No. 46-7002 or equivalent — see text) with K as ordinate.

2. Position this overlay so that its curve best fits the data while keeping the axes of the overlay parallel with the axes of the paper.

3. f is the value of Y at the point where the abscissa = 1 line of the overlay crosses the Y axis.

4. f $\sqrt{\pi\rho}$ is one tenth of the value of K where the ordinate = 10 line of the overlay crosses the K axis.

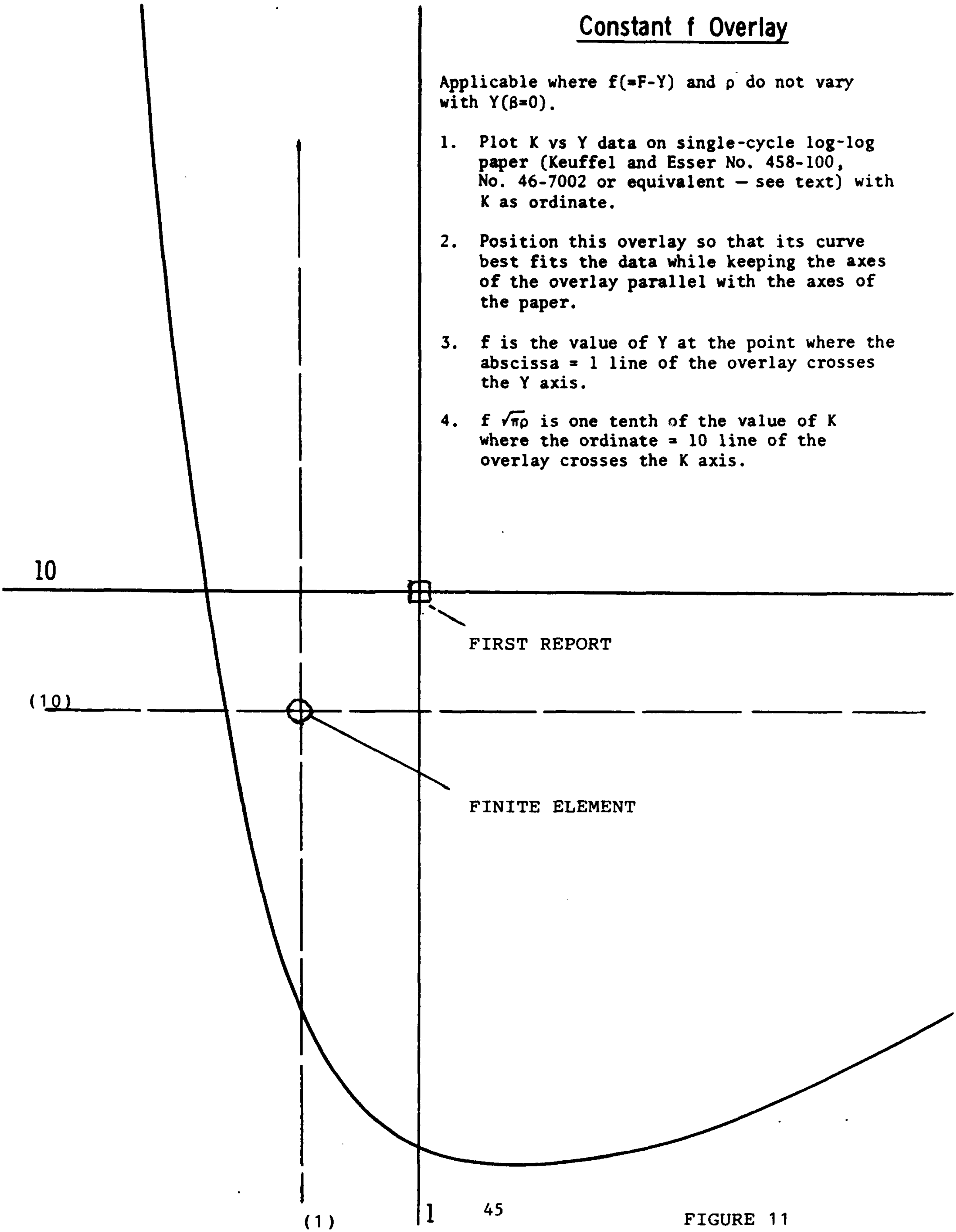

FIGURE 11

Constant F Overlay

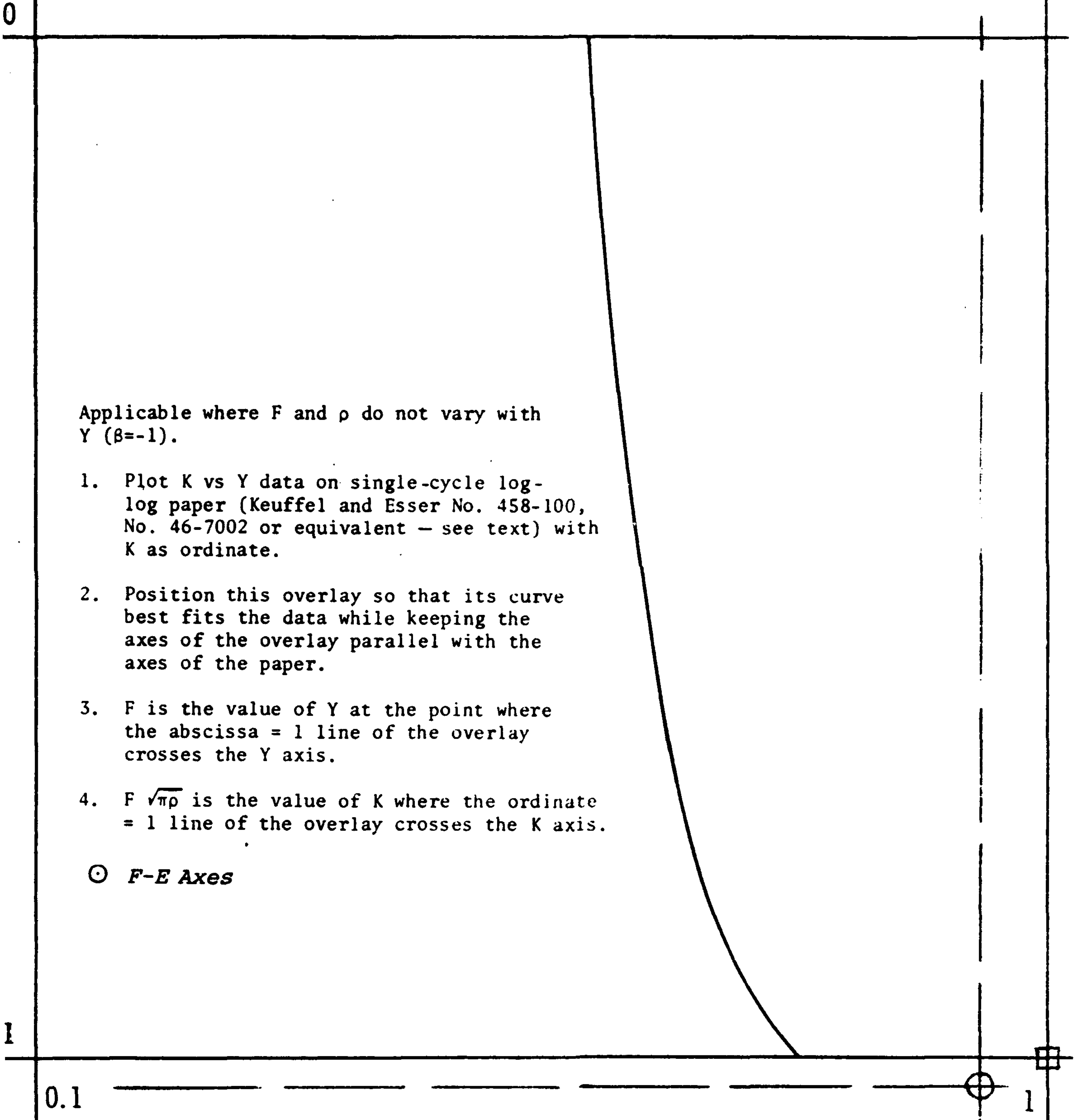

Applicable where F and ρ do not vary with Y (β=-1).

1. Plot K vs Y data on single-cycle log-log paper (Keuffel and Esser No. 458-100, No. 46-7002 or equivalent – see text) with K as ordinate.

2. Position this overlay so that its curve best fits the data while keeping the axes of the overlay parallel with the axes of the paper.

3. F is the value of Y at the point where the abscissa = 1 line of the overlay crosses the Y axis.

4. F $\sqrt{\pi\rho}$ is the value of K where the ordinate = 1 line of the overlay crosses the K axis.

FIGURE 12

APPENDIX I

TRANSPARENT OVERLAYS

The transparent overlays are made to be used repeatedly until worn out so long as it is desired to determine fracture stress and effective crack tip radius by use of them from yield strength and corresponding K_{Ic} measurements.

The overlays contain a curve, or curves, each identified by a parameter which conveys their relationship to a law relating fracture stress to yield strength. The curves are log-log plots of a purely mechanical stress analysis relationship existing between K_{Ic} yield strength, modulus of elasticity, Poisson's ratio, fracture stress, and effective crack tip radius, though expressed simply in terms of dimensionless groupings of these variables called L and Λ and expressed as L versus Λ. This relationship is insufficient in itself to determine fracture stress and radius in the absence of a fracture stress law relating fracture strength to yield strength and also a relation, here assumed to be determined experimentally, between K_{Ic} and yield strength.

In use the overlay is laid upon a log-log plot* of experimental or slightly modified experimental K_{Ic} versus Y data, in such a way as to best match the data in all or part of its

*To the same scale used in constructing the overlay, Figures 11 & 12 may be used as transparent overlays using a good back light.

range. In this position, the values of K and Y under the unit coordinate lines of the overlay yield the desired values of fracture stress and radius, as described below. The match must include at least three experimental points, for at least three points are necessary to establish curvature which, of course, describes the shape of a curve with a continuous slope.

The overlay curves themselves are constructed from a table of L versus Δ for assumed constant values of the fracture law parameter which is designated here by β and covers a practical instructive range of $-2 \le \beta \le 1$ for the fracture law used here. The curves are graphs of $\log 1/(\Delta - \beta)$ versus $\log 1/[(\Delta - \beta)L]$ and are easily transferred to transparencies by a number of copy machines.* The curves are interpreted in terms of fracture stress and radius.

Here, as always, the fracture stress is

$$F = Y + Y\Delta$$

so that

$$\Delta = \frac{F - Y}{Y}$$

---

*For example, a 3-M Thermofax Copier.

The fracture stress law is assumed to be linear in the K_{Ic}, Y region being matched; i.e.,

$$F = (1+\beta)Y + f$$

so that

$$\beta = \frac{F-Y}{Y} - \frac{f}{Y} = \Delta - \frac{f}{Y}$$

and, hence, $\Delta - \beta = f/Y$

The abscissa on the transparency is

$$\log 1/(\Delta-\beta) = \log Y/f = \log Y - \log f$$

so that Y = f where Y/f = 1 and log Y/f = log $1/(\Delta - \beta) = 0$.

The ordinate is

$$\log 1/[(\Delta-\beta)L] = \log[(Y/f)(K/Y\sqrt{\pi\rho})]$$

$$= \log K - \log f\sqrt{\pi\rho}$$

and

$$K = f\sqrt{\pi\rho} \textit{ where } 1/[(\Delta-\beta)L] = 1$$

Thus, if one of the β curves of the transparent overlay can be matched to a log-log plot of experimental values of K_{Ic} versus Y, the value of the Y intersected by the unit coordinate line of the overlay will be Y = f, for what is log Y on the plot is [log Y - log f]; i.e., 0 on the overlay when it is in the matching position. Correspondingly and similarly, the horizontal unit coordinate line of the overlay is where $K = f\sqrt{\pi\rho}$ and from this $\sqrt{\pi\rho}$ is derived by dividing out the value of f. Therefore, $\sqrt{\pi\rho}$ as well as the constants β and f of our fracture law are known.

The overlays and graphs for the examples in the First Report were for $\beta = 0$; i.e., F = Y + f, and $\beta = -1$ (i.e., F = f, independent of Y). The curves for making these overlays and the experimental data were plotted on the largest size single cycle log-log paper locally available that would fit into this report with K on the vertical and Y on the horizontal scale. This size paper and the corresponding overlays are considered so generally useful that such overlays are included in this report and are called the f (for $\beta = 0$) and F (for $\beta = -1$) overlays.

However, to make an overlay to cover the larger range of experimental variables and ranges of β that may be encountered, 2 x 3 log-log paper, whose size also conforms to that of the report had to be used. Unlike the scale of the single cyle paper above, this selection of paper means that for this wider range the scale is such that the Y values (plotted on the horizontal axis, as before) increase from right to left.

APPENDIX II

ENERGY RELATIONS IN SUPERPOSITION OF HYDROSTATIC PRESSURE

In view of the fact that, in contrast to three-dimensional problems, in plane strain a lateral stress is required to keep the thickness constant, and in plane stress there is no lateral stress, it may be wondered just how the superposition of hydrostatic pressure is to be carried out (whether lateral pressure is to be employed). Here the superposition is taken in such a way as to preserve the plane strain and stress conditions. Thus, to modify the general expression for energy per unit volume in terms of the stresses for the inclusion of hydrostatic pressure, p:

- for three dimensions add - p to each stress

- for plane stress make the stress in the thickness direction zero and add nothing to it

- for plane strain make the stress in the thickness direction $\sigma\ (\sigma_x + \sigma_y)$ in which σ without a subscript is Poissons's ratio, and add p to σ_x and to σ_y, including the σ_x and σ_y in $\sigma(\sigma_x + \sigma_y)$.

Each modified expression for energy is the integrand of an integral over the volume of a body for the total energy of that body; the part, in each case, without p is the whole energy before superposition of p and the part containing terms in p is the decrease in energy caused by superposition of pressure p. The latter consists of a simple term in p^2 and a part in which the sum of the original stresses is multiplied by p. By replacing each such stress by its isotropic Hooke's Law expression of the type $\sigma = \lambda\Delta + 2\mu\varepsilon$, it is seen that the sum represents the unit dilatation so that the integral of this part is a constant multiplied by $p\int\Delta dV$, i.e., pressure multiplied by the whole dilatation caused by the original stresses.

This dilatation was produced by an original exterior boundary loading stress + p since this is the p that is being eliminated on the exterior boundary by the hydrostatic addition of -p. The total dilatation $\int\Delta dV$ above is expressed in terms of the original loading stress +p by means of a theorem in Love's "The Mathematical Theory of Elasticity", Article 123.

It is found that (since the crack has no volume in the unstrained condition) the total energy contribution caused by the hydrostatic -p addition is:

- for three dimensions $-p^2V/2K$

  Where the bulk modulus $K = E/[3(1 - 2\sigma)]$
- for plane stress $-p^2 V/2K_1$

  where the bulk area modulus $K_1 = E/[2(1 - \sigma)]$
- for plane strain $-p^2V/2K_2$

  Where the bulk area modulus $K_2 = E/[2(1 - \sigma)\ (1 - 2\sigma)]$

as though there was no crack at all.

Where hydrostatic pressure cancels the external load leaving the crack under internal pressure, these simple terms are the amounts the total original energy has decreased; what energy remains, since the only load is now in the crack, is due to that pressure in the crack. This energy, because displacement in the crack is proportional to the internal pressure, is the pressure multiplied by half the volume it produces.

Now, consider from this background of superimposed hydrostatic stress, Griffith's analytical difficulty. He states, "A solution of this problem was given in a paper read in 1920 but in the solution there given the calculation of the strain energy was erroneous in that the expression used for the stresses gave values at infinity differing from the postulated uniform stress at infinity by an amount which, though infinitesimal, yet made a finite contribution to the energy when intregated around the infinite boundary. This difficulty has been overcome by slightly modifying the expressions for the stresses, so as to make this contribution to the energy vanish, and the corrected condition for the rupture of a thin cracked plate under a uniform pull applied in its plane at its outer edge is $R=\sqrt{2ET/\pi c}$ where...".[4]

Now suppose we have a plate containing a crack (or a hole for that matter) under internal pressure p only, superposition of a hydrostatic tension p on that plate will eliminate the internal pressure p and load the plate on its outer edge with a tension stress acting normally to its outer edge; there are no secondary stresses even though no limit has been put on the size or shape of the plate. Any energy input caused by the presence of a crack is due to the action of the original internal pressure on the sides of the crack. Within reason, it would seem that little error in this energy input would be made if the maximum opening of the crack is considered known, if the crack is assumed to have gone into an elliptical shape even where this is not the case; e.g., if the cracked plate is short or narrow in comparison to the size of the crack.

REFERENCES

1. BEEUWKES, R., Jr. "Analysis of Failures," Proceedings of the Third Sagamore Ordnance Materials Research Conference, Analysis of Failures, Duke University, 5-7 December 1956, p. 89-163. Printed by Syracuse University Research Institute (Correction: Multiply $(N - N_0)$ by $(3/4)^{1/3}$.

2. BEEUWKES, R., Jr. "Characteristics of Crack Failure," Surfaces and Interfaces, v. II, Syracuse University Press, Syracuse, NY, 1968.

3. BEEUWKES, R., Jr. "On Status of Correlation of Crack Failure with Material Properties in Metals," U.S. Army Research Laboratory, AMMRC TN 69-01, March 1969.

4. BEEUWKES, R., Jr., HANSEN, A. M., and TREMBLAY, R. J. "Determination of Fracture Stress and Effective Crack Tip Radius from Toughness (K_{Ic}) and Yield Strength (Y)," U.S. Army Research Laboratory, AMMRC TR 78-44, October 1978.

5. KOBAYASHI, A. S., CHIU, S. T., and BEEUWKES, R., Jr. "Elastic-Plastic State in a Plate With an Extending Crack," Proceedings of the Army Symposium on Solid Mechanics - 1970, Lightweight Structures: also U.S. Army Research Laboratory, AMMRC MS 70-5, v. IV, December 1970.

6. KOBAYASHI, A. S., CHIU, S. T., and BEEUWKES, R., Jr. "Elastic-Plastic State and Fracture of a Blunt Notched Tension Plate," in Mechanical Behavior of Materials. The Society of Materials Science, v. 1, Japan, 1972, p. 446-457.

7. TRACEY, D. M., and FREESE, C. E. "Plasticity Near a Blunt Flaw Under Remote Tension," ASTM STP 995, 1989, p. 93-106.

8. TRACEY, D. M., and FREESE, C. E. "Importance of Crack Tip Shape in Elastic-Plastic Fracture Analysis," Proceedings of the Second Army Conference on Applied Math and Computing," 1985, p. 359-371, U.S. Army Materials and Mechanics Research Center, Watertown, MA.

9. KE, J. S., and LIU, H. W. "Thickness Effect on Crack Tip Deformation at Fracture," Syracuse University, Contract Number DAAG46-73-C-0209, Final Report, AMMRC CTR 74-57, Volume IV, December 1976.

10. KE, J. S., and LIU, H. W. "The Measurements of Fracture Toughness of Ductile Materials," Presented at the Symposium on Fracture and Fatigue, George Washington University, Washington, DC. Pergamon Press, Oxford, NJ, 1972.

11. GRIFFITH, A. A. "The Theory of Rupture," Proceedings of the International Congress for Applied Mechanics, Delft, Holland, 1924.

12. GRIFFITH, A. A. "The Phenomena of Rupture and Flow in Solids," Phil. Trans. Roy. Soc. London, A., v. 221, 1921, p. 163-198.

13. TAGGART, R., and WAHI, K. K. "Crack Opening Displacement During the Tensile Loading of Ductile and Brittle Notched Plates," University of Washington, Seattle, under subcontract to Syracuse University Prime Contract DA-31-124-ARO(D)-112, Final Report, AMMRC CTR 72-33, February 1972; also, abridged version entitled "The Relationship between the Fracture Toughness and the Crack Tip Radius," by TAGGART, R., WAHI, K. K., and BEEUWKES, R., Jr., ASTM STP 605, 1976, p. 62.

14. GARDE, A., and WEISS, V. "Brittle Fracture Initiation at the Elastic-Plastic Interface," Syracuse University Research Institute, Contract DA-31-124-ARO(D)-112, Interim Technical Report, AMMRC-CR 70-29, February 1970; also, "Brittle Crack Initiation at the Elastic-Plastic Interface," Met. Trans. AIME, v. 3, November 1972, p. 2811.

15. BEEUWKES, R., Jr. "Stresses in Thick Walled Cylinders," presented at the International Congress for Applied Mechanics, Paris, France, 10 October 1946. Watertown Arsenal Laboratory Report WAL 730/419, 1946.

16. SMITH, J. H. "Some Experiments on Fatigue of Metals," Journal of the Iron and Steel Institute, September 1910, p. 246-318.

17. SMITH, J. H., and WEDGEWOOD, G. A. "Stress-Strain Loops for Steel in the Cyclic State," Journal of the Iron and Steel Institute, 1915, p. 365-397.

18. BATSON, R. G., and HYDE, J. H. "Mechanical Testing," The D. U. Technical Series, published by E. P. Dutton, p. 224-226

19. BECHTOLD, J. H., and SHEWMON, P. G. "Flow and Fracture Characteristics of Annealed Tungsten," Trans ASM, v. 46, 1954, p. 403 (See Figure 8).

DISTRIBUTION LIST

No. of Copies	To
	Director, U.S. Army Research Laboratory, 2800 Powder Mill Road, Adelphi, MD 20783-1197
1	ATTN: AMSRL-OP-CI-AD, Technical Publishing Branch
1	AMSRL-OP-CI-AD, Records Management Administrator
	Commander, Defense Technical Information Center, Cameron Station, Building 5, 5010 Duke Street, Alexandria, VA 23304-6145
2	ATTN: DTIC-FDAC
	Commander, U.S. Army Materiel Command, 5001 Eisenhower Avenue, Alexandria, VA 22333
1	ATTN: AMCSCI
	Director, U.S. Army Research Laboratory, Watertown, MA 02172-0001
2	ATTN: AMSRL-OP-WT-IS, Technical Library
5	Author